energies

MDPI

Article

Evaluation of the Effects of Smart Charging Strategies and Frequency Restoration Reserves Market Participation of an Electric Vehicle

Fabian Rücker [1,2,3,4,*], Michael Merten [1,2,3], Jingyu Gong [1,2,3], Roberto Villafáfila-Robles [4], Ilka Schoeneberger [1,2,3] and Dirk Uwe Sauer [1,2,3,5]

1 Chair of Electrochemical Energy Conversion and Storage Systems, Institute for Power Electronics and Electrical Drives (ISEA), RWTH Aachen, Jägerstr. 17–19, 52066 Aachen, Germany; michael.merten@isea.rwth-aachen.de (M.M.); jingyu.gong@isea.rwth-aachen.de (J.G.); ilka.schoeneberger@isea.rwth-aachen.de (I.S.); sr@isea.rwth-aachen.de (D.U.S.)
2 Juelich Aachen Research Alliance, JARA-Energy, 52062 Aachen, Germany
3 Institute for Power Generation and Storage Systems (PGS), E.ON ERC, RWTH Aachen University, 52074 Aachen, Germany
4 Centre d'Innovació Tecnològica en Convertidors Estàtics i Accionaments (CITCEA-UPC), Departament d'Enginyeria Elèctrica, ETS d'Enginyeria Industrial de Barcelona, Universitat Politècnica de Catalunya, Avinguda Diagonal, 647, Pl.2, 08028 Barcelona, Spain; roberto.villafafila@citcea.upc.edu
5 Ionics in Energy Storage (IEK-12), Helmholtz-Institute Münster (HI MS), 48149 Münster, Germany
* Correspondence: fabian.ruecker@isea.rwth-aachen.de or fabian.rucker@upc.edu

Received: 2 May 2020; Accepted: 8 June 2020; Published: 16 June 2020

Abstract: The emergence of electric vehicles offers the opportunity to decarbonize the transportation and mobility sector. With smart charging strategies and the use of electricity generated from renewable sources, electric vehicle owners can reduce their electricity bill as well as reduce their carbon footprint. We investigated smart charging strategies for electric vehicle charging at household and workplace sites with photovoltaic systems. Furthermore, we investigated the participation of an electric vehicle in the provision of positive automatic frequency restoration reserve (aFRR) in Germany from 30 October 2018 to 31 July 2019. We find that the provision of positive aFRR in Germany returns a positive net return. The positive net return is, however, not sufficient to cover the current investment cost for a necessary control unit. For home charging, we find that self-sufficiency rates of up to 48.1% and an electricity cost reduction of 17.6% for one year can be reached with unidirectional smart charging strategies. With bidirectional strategies, self-sufficiency rates of up to 56.7% for home charging and electricity cost reductions of up to 26.1% are reached. We also find that electric vehicle (EV) owners who can charge at their workplace can reduce their electricity cost further. The impact of smart charging strategies on battery aging is also discussed.

Keywords: electric vehicle; smart charging; self-consumption; self-sufficiency; aFRR; frequency restoration reserve; grid service; battery aging; prosumer; photovoltaics

1. Introduction

The Paris Agreement aims to hold the increase in the global average temperature to well below 2 °C. Party members of the agreement should foster climate resilience and low greenhouse gas (GHG) emissions development with developed country parties taking the lead by undertaking economy-wide absolute emission reduction targets [1]. The EU ratified the agreement on the 4th of November 2016 and has since then set GHG reduction targets in order to comply to the agreement. In Germany, the Renewable Energy Sources Act EEG aims to increase the share of renewable energies in the electricity

generation sector. The share of renewable energies reached 40% in 2018 and the photovoltaic share reached 8% (45.75 TWh) [2]. Most photovoltaic (PV) systems in Germany are operated by private individuals and farmers and more than 98% are installed in the low-voltage grid [3]. In addition to the electricity generation sector, other sectors such as the heating and the transportation sectors have to be decarbonized. In the transportation sector, battery electric vehicles (EVs) can provide this reduction as these vehicles can be powered by electrical energy generated from renewable energies. Fuel cell vehicles and conventional combustion engine vehicles can also be operated carbon-free if their fuel is synthesized via a power-to-fuel process using renewable sources. However, the efficiency of these processes is still comparatively low, whereas the electrical energy can be used directly in an EV. Pushed by EV friendly legislations and financial incentives, an increasing number of electric vehicles (EVs) are on the road in Germany, Europe, and worldwide. In order to unlock the full potential of these trends, the electrical energy demand of EVs should ideally be matched with the supply of renewable energy. For household installations with PV systems (prosumer households) different approaches have been studied in order to match the PV generation and the household load have been studied. One approach is the use of a battery energy storage system (BESS) to store electricity generated by the PV system. The use of PV BESS is incentivized by a funding scheme of the KfW Group, a German banking group focused on economic development [4]. Various studies have investigated the use of a PV BESS to increase the self-consumption of PV energy and the self-sufficiency of a household. In [5], the authors studied different operation strategies that also use forecasts. They found that the levelized cost of electricity can be reduced by up to 12%. Another study optimized the optimal PV battery home storage system size for households in the Dutch city of Amersfoort and assesses the peak shaving potential for different charging strategies [6]. Under the assumption that excess PV energy injected to the grid is not reimbursed (pure self-consumption policy), the work in [7] shows that under current market prices a PV system coupled with a BESS is not profitable. Other studies have investigated the impact of the introduction of EVs on prosumer households. In [8], the authors use a stochastic model to illustrate that the self-consumption of PV power can be increased by the introduction of EVs which charge upon arrival at the household. In [9], the authors conduct a techno-economic analysis of Vehicle-to-Home (V2H) charging strategies in prosumer households. The study shows promising results with an 11% cost reduction due to the addition of the V2H strategy.

In Germany the phase-out of conventional thermal power plants is underway such as the phase-out of nuclear power plants in Germany by 2022 (§7 Section 1a AtG) and the planned phase-out of lignite-fired power plants by 2038. These power plants will not be available in the future to provide ancillary services such as Load Frequency Control (LFC). The provision of LFC by other means is therefore a current research field. In [10], the authors show that the control of static and motor type smart loads can collectively offer a short-term power reserve which is comparable to the spinning reserve in the Great Britain system. In [11], the authors found that the combination of PV self-consumption with the provision of Frequency Restoration Reserve (FRR) with PV BESS leads to profitable investments. Furthermore, large stationary storage systems are increasingly set-up to provide LFC services, especially Frequency Containment Reserve (FCR), such as a 5 MWh/5 MW battery system in Aachen, Germany [12]. In addition, renewable energy generators are pooled together with energy storage systems to provide LFC [13,14]. Moreover, EVs participate in pilot projects to provide FCR [15,16]. Previous studies have also studied the participation of EVs and BESSs in the FRR market are difficult to compare as the market and auction design has changed frequently over the last years. In [17], the authors found "that it is not economically beneficial to provide aFRR (automatic Frequency Restoration Reserve) with a standalone battery" (Olk et al. P.1 [17]). Moreover, the participation in the market for negative aFRR of integrated homes with PV BESS combined with a heat pump for power-to-heat coupling has been studied. The authors found that the annual costs for heat and electricity can be reduced by 14.5% [18]. The study conducted in [19] found that the participation of EVs providing negative aFRR leads to profits that are too low to offer an incentive for buying an EV and that the available battery capacity is the decisive bottleneck.

In this study, we extend V2H charging strategies towards Vehicle-to-Grid (V2G) charging strategies to provide a Load Frequency Control service to the grid. We investigate the provision of positive aFRR of an EV integrated into a prosumer household with a PV system. This is particularly interesting as the number of EVs is increasing and with it the energy and power capacity available to the grid. In the last quarter of 2019 the daily demand for aFRR was in the range of 1911 MW (positive) and 1808 MW (negative) [20]. Due to the small size of the market and the expected number of EVs, the provision of aFRR with EVs could have a great impact on the market.

We compare the positive aFRR provision to other smart charging strategies that aim to maximize the self-consumption of PV energy and the self-sufficiency of the prosumer household. Furthermore, we investigate the impact of the charging strategies on the grid and the EV traction battery. This study is carried out in the German context (geographical, legislation, etc.), but as the market harmonization and coupling in continental Europe is ongoing, the results are widely applicable.

2. Load Frequency Control

In the electrical grid, load and power generation have to be balanced at all times to establish a stable and reliable grid operation. It is the Transmission System Operators' (TSO) responsibility to maintain this balance. Before the energy delivery is activated the balance responsibility is passed on to Balance Responsible Parties (BRPs) [21]. The match of supply and demand is done on electricity markets. This is a continuous process with the existence of different electricity markets which differ in the lead time between the moment of trade and of delivery. On forward and future markets, electrical energy can be traded years before the day of delivery. On the day-ahead markets energy is traded one day before delivery and on the continuous intra-day markets, market participants can correct energy imbalances on the actual day of delivery (down to 5 min before delivery in the case of Germany on the EPEX Spot market [22]). Even after the clearing processes of the markets, imbalances of demand and supply of electrical energy can occur during real-time operation due to outages of power plants and errors in the forecast of load and power generation. Here balancing markets come into play which can be split into procurement (i.e., procurement and activation of reserves by the TSO) and settlement (i.e., financial settlement of the BRP imbalances by the TSO). Four different balancing reserves with individual technical requirements are defined following the Network Code on Load-Frequency Control of ENTSO-E [23].

1. Frequency Containment Reserve (FCR)
2. automatic Frequency Restoration Reserve (aFRR)
3. manual Frequency Restoration Reserve (mFRR)
4. Replacement Reserve (RR)

Figure 1 illustrates the order of activation of balance reserves in the case of an imbalance and the responsible areas of the Load-Frequency Control (LFC) process. From left to right the requirements on response time, ramp rates, and the level of automated activation become less stringent, with FCR having the most stringent requirements. In the European continental (CE) synchronous area, FCR is activated non-selectively to stabilize the frequency within seconds when an imbalance between load and generation occurs. For the CE synchronous area, the jointly dimensioned amount of FCR power is 3000 MW in positive direction and negative direction [24]. In Germany the call for tenders for FCR and aFRR is jointly organized by the German TSOs on the internet platform regelleistung.net. In addition to the German TSOs 50hertz, Amprion, Tennet, and TransnetBW, the Austrian TSO APG also participates since July 2016. The TSOs are also part of the International Grid Control Cooperation (IGCC) in order to avoid contradicting procurement of FRR by imbalance netting. In this study, we focus on the procurement and activation of aFRR by TSOs.

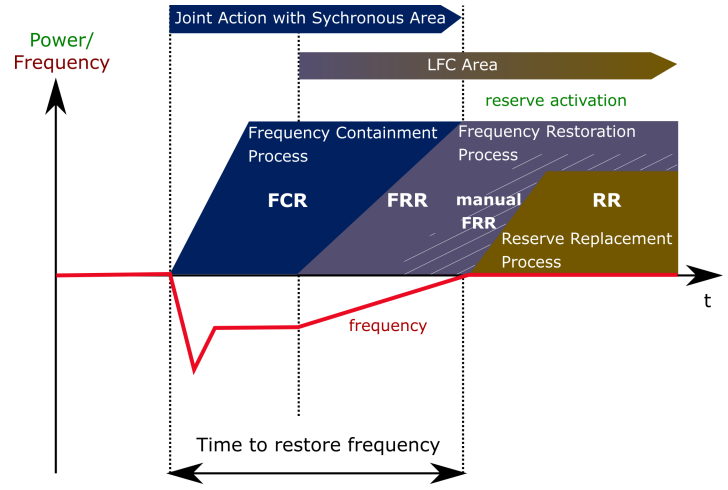

Figure 1. Hierarchy of Load-Frequency-Control (under assumption that Frequency Containment Reserve (FCR) is fully replaced by Frequency Restoration Reserve (FRR). FRR is commonly divided into automatic frequency restoration reserve (aFRR) and manual FRR.

2.1. Frequency Restoration Reserve (FRR)

Whereas FCR must be fully activated within 30 s, automatic Frequency Response Reserve (aFRR) must be fully activated within 5 min and manual Frequency Response Reserve (mFRR) within 15 min after an event causing an imbalance [25]. This study focuses on aFRR, which is also referred to as Secondary Control Reserve (SCR). In order to be prequalified for the aFRR market, the technical unit must be capable of generating a measurable power output after 30 s, deliver the full tendered power within 5 min, and provide the full tendered power for 4 h. The TSOs adjust the total aFRR demand (in MW) for their respective control zone [25]. Prequalified units are allowed to participate in a multi-unit, open, pay-as-bid, anonymous, and transparent auction process. Daily auctions are held for six different time slices and positive and negative delivery directions (see Figure 2).

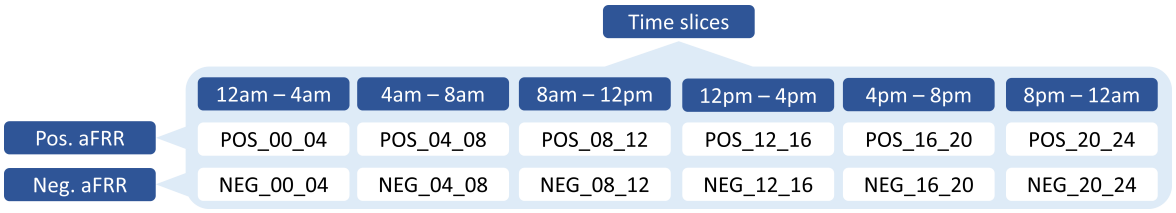

Figure 2. Time slices of products in the considered FRR market design (October 2018–July 2019) [26].

Participants can submit a bid tuple with the capacity (MW), capacity price (€/MW) and energy price (€/MWh) for each product type. The participants are awarded either based on the capacity price or on the mixed price depending on the auction scheme. In this study, the mixed price auction scheme is considered, which served as the auction scheme from October 2018 to July 2019. The mixed price for each product (B_{MP}) is based on the submitted capacity price (B_C), the submitted energy price (B_E) and a factor (a_M) published quarterly by the TSOs (see Equation (1)).

$$B_{MP} = B_C + a_M \cdot B_E \tag{1}$$

All submitted bids are ordered by mixed price (merit order) by the TSOs. The cheapest bids are accepted until the total aFRR demand is fulfilled. Awarded participants will be remunerated with the capacity price bid by them, even if they do not get activated to provide aFRR power. Awarded participants are remunerated with the energy price bid once they get activated and provide aFRR power. In the case of grid imbalances that have not been equilibrated by FCR, the activation of participants starts with the one with the lowest energy bid until the aFRR power demand is met. The position in the

merit-order list of energy price bids determines the frequency of activation of participants. The capacity of the traction battery of the EV is too small to participate in the aFRR market as a standalone unit due to the minimum bid size of 1 MW. Therefore, we assume that the EV is integrated into a pool of EVs and storage units. Furthermore, we assume a perfect forecast for the availability of pool capacity. Due to the complexity of the auction, the bidding strategy of a participant is not trivial. In this publication, we consider a bidding strategy that has been developed in [26] for a 20 MWh/20 MW stationary battery storage system (Li-Ion NMC). EVs are also commonly powered with traction batteries with a Li-Ion NMC chemistry and therefore share similar technical requirements. The bidding strategy is based on an optimization approach to derive an optimal bid and to estimate the revenue potential on the market. An optimal bid is obtained by involving an aFRR market prediction tool [27] and by estimating expected differential battery aging costs as a function of the individual aFRR energy price. In Figure 3, one week of the resulting aFRR bids (capacity and energy price) and aFRR activations (requested) is shown as well as the weighted average price of the intraday market. The blue line of "aFRR offered" shows the awarded capacity. The pool receives the power capacity remuneration (B_C) for these slots. The power capacity price is not shown and not considered in this study as it is negligible for a single EV in a pool. The red area shows the power that is requested. The pool receives a remuneration (B_E) for the energy provided for aFRR. The energy that the EV discharges in order to provide aFRR has to be recharged before departure. An order on the intraday market is placed to recover the provided energy and the efficiency losses. The difference between the aFRR energy price and the intraday price, plus an additional grid fee, is the operational margin of profit for the aFRR provision. During the period of 30 October 2018–31 July 2019, the pool offering aFRR is awarded the participation for 916 out of 1638 possible 4 h time slots. During 503 timeslots out of the awarded 916 the pool is activated and needs to provide aFRR.

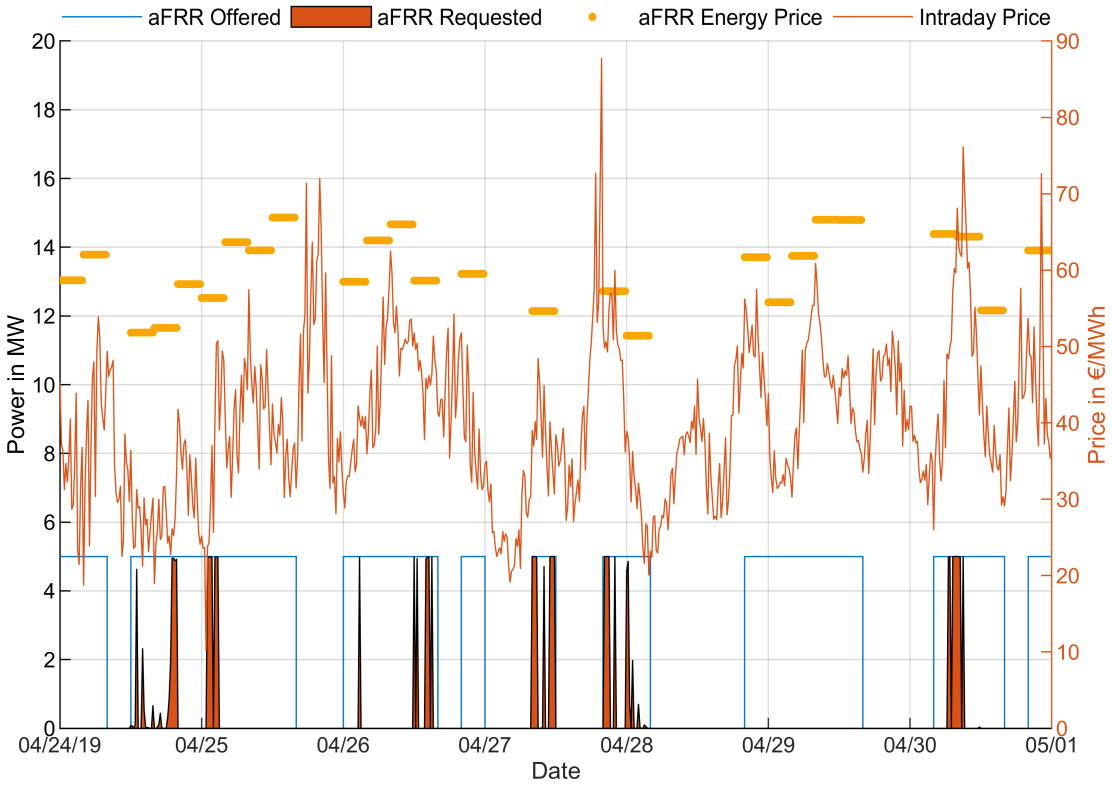

Figure 3. The diagram shows on the left *y*-axis the power capacity offered and awarded for aFRR, the aFRR power that was requested. On the right *y*-axis the energy prices for aFRR and the intraday market are shown.

2.2. Modeling and Methods

In this publication, we carry out power-flow simulations of prosumer households using Matlab®/Simulink. The simulation considers active power and does not consider reactive power, harmonics or phenomena of multiphase systems such as asymmetric loading. Furthermore, we do not model highly dynamic processes on a scale of smaller than 1 s. The input data of the model has a resolution of 1 min.

Model Setup and Components

The prosumer household consists of a PV system, an EV with a charger (converter), inflexible household load (lights, cooking, washing, leisure, etc.), and a connection to the grid. The charger is unidirectional or bidirectional depending on the simulated scenario. The structure of the modeled system is illustrated in Figure 4 and the relevant parameters are summarized in Table 1.

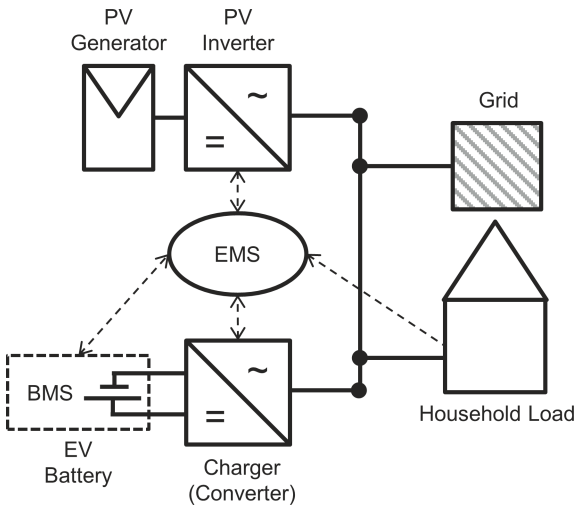

Figure 4. Schematic of the simulation model. The solid lines show the power flow and the dashed lines show the information flow. The main information systems are the Energy Management System (EMS) and Battery Management System (BMS).

Table 1. Summary of the characteristics of the EV, the PV system, and the household load.

Electric Vehicle		PV System		Household	
P_{Motor}	125 kW	$P_{PV\,Panel}$	10 kW_p	Persons	4
$C_{Battery}$	38 kWh	$P_{PV\,Inverter,AC-Link}$	7 kW	$E_{consumption}$	4274 kWh/a
$C_{Battery,usable}$	35.4 kWh	$\phi_{Azimuth}$	0° (south)		
SoC Range	3.2–95.3%	$\beta_{inclination}$	30°		
Battery layout	93S1P	$E_{gen,AC-Link}$	9734 kWh/a		
C_{cell}	110.8 Ah				
Annual Driving Distance	*Worker*: 14,743 km *Late-Worker*: 14,924 km *2nd Car*: 10,211 km				
$P_{charger,peak}$	10 kW				

The PV generator and the PV inverter model have been developed and published in [28] and described in greater detail in [29]. We set the sizing of the PV panels, MPP tracker, and inverter according to the most common installation portfolio for the segment of households in Germany. The size of the installed PV systems does not solely depend on the available installation space. Due to the decreasing prices of PV systems, the size of PV systems on households has increased in the last years [30]. Furthermore, the regulatory framework has an impact on the size of installed PV systems. According to the Renewable Energy Sources Act (EEG 2017) in Germany, the installation operator of an

electric energy production system in which only renewable energy sources are used, has an entitlement to claim from the grid operator for the electricity generated (§ 21 EEG). For households the claim is commonly a feed-in tariff. The feed-in tariff depends on the installed capacity of the installed system and the date of commission of the system. In this publication, we chose the first half of the year of 2018 as the commission date of the PV system. The corresponding feed-in tariff is 0.1220 €/kWh for a PV system up to 10 kWp. PV systems commissioned in the first half of 2018 with a peak power of more than 10 kWp and less than 40 kWp have a lower feed-in tariff of 0.1187 €/kWh [31]. Furthermore, operators of a PV system of up to 10 kWp are exempt from the EEG surcharge on self-consumption of generated electricity (§ 61a EEG). Due to these regulations, PV systems with a peak power of 10 kWp make up a large portion of the PV systems installed recently [30]. Therefore, we choose a peak power of 10 kWp for the PV systems in this publication. The EEG also states technical requirements for PV installations. PV systems with an installed capacity of over 30 kWp must be equipped with a shared technical device which the grid system operator can use at all times to reduce the entire feed-in by remote control. This is done in the event of grid system overload or to call up the current level of total feed-in. PV systems below 30 kWp are exempt from this, if the maximum effective capacity fed in at the point of connection of their installation with the grid system is limited to 70% of the installed capacity (§ 9 EEG). In this publication, the peak power output of the PV system is limited to 70% of the peak power rating on the AC side. The rated PV power is set to 10 kWp for our simulations, whereas the peak power output of the PV inverter is set to 7 kW. In the case that the PV system could generate more than 7 kW of power output to the grid, energy is lost as the PV inverter is limited to an output power of 7 kW. However, the energy loss annually is only 2% as the PV system is seldom able to generate more than 70% of its rated peak power at the considered location, Lindenberg (Tauche, Germany). The PV panel model, based on the work in [32], calculates the DC power and voltage output at the maximum power point. The input data is irradiation data in form of global, diffuse and beam irradiation. Also, a temperature profile as a thermal model of the PV panel is implemented. In this publication, the radiation data, used as input, was measured in Lindenberg (Tauche, Germany), close to Berlin, in the year 2006 [33]. The energy management system (EMS) controls the set point of the EV charger. The battery management system (BMS) controls the power flows in the EV. The BMS sets the maximum charging power of the battery and communicates it to the EMS. The inflexible load is modeled using load profiles of German households based on real data measurements [34]. The household in this publication is based on a 4-person household with a yearly consumption of 4274 kWh.

The EV battery model and charger are based on the Smart electric drive (3rd Generation [35], production year and manufacturer: 2013, Daimler AG). The traction battery of the Smart electric drive (2013) has a battery layout of 93s1p. We scale the original cell capacity of 52 Ah to 110.8 Ah, which results in an EV with a capacity of 38 kWh. Doing this ensures that the voltage level of the battery remains the same. The BMS limits the usable range of the state of charge (SoC) to 3.2–95.3%. The usable battery capacity is therefore 35.4 kWh. EVs that feature this capacity are the BMW i3 and the Nissan Leaf in 2019. We therefore set the motor power to 125 kW, which corresponds to a BMW i3.

When the EV is charging at the workplace, the workplace is simulated in the same way as the household with the same components shown in Figure 4. The PV system of the workplace is characterized by $P_{PV\,Panel,workplace} = 30\,\text{kW}$ and $P_{PV\,Inverter,workplace} = 21\,\text{kW}$ with the same azimuth and inclination angles as the household system. The load profile of the workplace is a profile of an office building with an annual consumption of 21,000 kWh.

2.3. Mobility Profiles

In this publication, each vehicle conducts zero or one round-trip per day. A round-trip starts with the departure of the EV from the household and ends with its arrival thereat. Depending on the scenario, the EV can be charged only at home, only at the company site or at both sites. Opportunity charging at public charging stations is not considered as it is not essential for the considered mobility profiles. We investigate different mobility profiles in order to investigate its impact on the self-sufficiency and

electricity costs of the household. The different mobility profiles are motivated by the assumption that the driver uses the vehicle to commute to and from work from Monday to Friday and leisure trips on the weekend. The profiles correspond to common mobility profiles for commuters in Germany [36]. We chose three mobility profiles that differ in the annual driving distance and the connection time during the day to the charging station. Especially the connection time during the day, is expected to have a significant impact on the electricity cost as it has an impact on the share of power generated by the PV system available to charge the EV. We therefore, chose mobility profiles with very different connection times during the day during workdays. Furthermore, a person in a 4-person household in Germany is not mobile on 8% of the workdays and 21% of the days on weekends [36]. This is taken into account in the mobility profiles in this publication as the EV is not used on days with no mobility and is assumed to be plugged in at the household. The departure times, arrival times, and the distances traveled are distributed for each profile following normal distributions. We set lower and upper limits for the mobility parameters that can not be undershot or exceeded respectively. The parameters of the normal distributions and the limits are summarized in Table 2 and visualized in Figures 5, 6, and A2. The profiles differ in the modes of the distributions for the arrival and departure times on workdays. On the weekend they all follow the same distributions. Profile *Worker* has a departure and arrival time mode of 6:45 h and 16:30 h at the household, respectively. The other profiles are *Late-Worker*, which is similar to *Worker* but with shifted departure and arrival times, and profile *2nd Car*, which is inspired by the use profile of a second car of a family household. The arrival windows for all profiles are broader than the departure windows due to the assumption that the driver aims to commute to and from work at the same time each workday but the arrival times have a greater variance due to the influence of traffic or detours. The driving profiles on the weekend are modeled following the same distributions for each profile. During weekends the probability density functions and the window widths for the departure and arrival times are broader than on workdays as the mobility pattern of the driver is assumed to be less regular. The mode of the normal distribution for the distance traveled on a workday is assumed to be larger than the mode for a day on the weekend. The probability density functions (PDFs) for the departure and arrival times are shown for workdays in Figure 5a, and for weekends in Figure 6a for the profile *Worker*. The PDFs for the daily driving distance are shown for workdays in Figure 5b for the profile *Worker*. The PDFs of the workday profiles *Late Worker* and *2nd Car* are shown in Figures A1 and A2. The distributions for the weekend which are the same among all three mobility profiles are shown in Figure 6. Mobility profiles *Worker* and *Late-Worker* have almost the same annual driving distance with 14,743 km and 14,924 km, respectively, while profile *2nd Car* has a lower annual driving distance of 10,211 km.

Table 2. Parameters of the normal distributions and limits for the mobility parameters departure time, arrival time, and driving distance.

Mobility Profile	Day	Parameter	μ	σ	Lower Limit	Upper Limit
Worker	**Workday**	Departure	6:45 h	0.1 h	6:30 h	7:00 h
		Arrival	16:30 h	0.5 h	16:00 h	17:00 h
		Distance	50 km	10 km	20 km	110 km
Late Worker	**Workday**	Departure	13:30 h	0.1 h	13:00 h	14:00 h
		Arrival	23:00 h	0.5 h	22:00 h	24:00 h
		Distance	50 km	10 km	20 km	110 km
2nd Car	**Workday**	Departure	9:00 h	0.1 h	8:30 h	10:30 h
		Arrival	13:30 h	0.5 h	12:00 h	15:00 h
		Distance	30 km	10 km	5 km	55 km
Worker, Late-Worker, 2nd Car	**Weekend**	Departure	10:30 h	5 h	8:00 h	13:00 h
		Arrival	18:30	5 h	14:00 h	23:00 h
		Distance	30 km	25 km	3 km	180 km

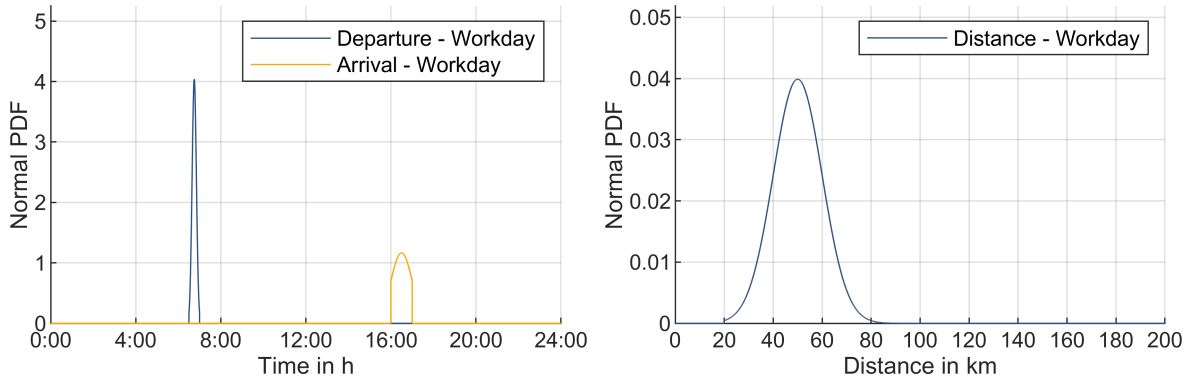

(**a**) (**b**)

Figure 5. Probability density functions (PDFs) of the driving profiles for mobility profile *Worker* on a workday. (**a**) PDF of the normal distribution used to model the departure and arrival times at home on a workday (Monday–Friday) for mobility profile *Worker*; (**b**) PDF of the normal distribution used to model the driving distance on a workday (Monday–Friday) for mobility profile *Worker*.

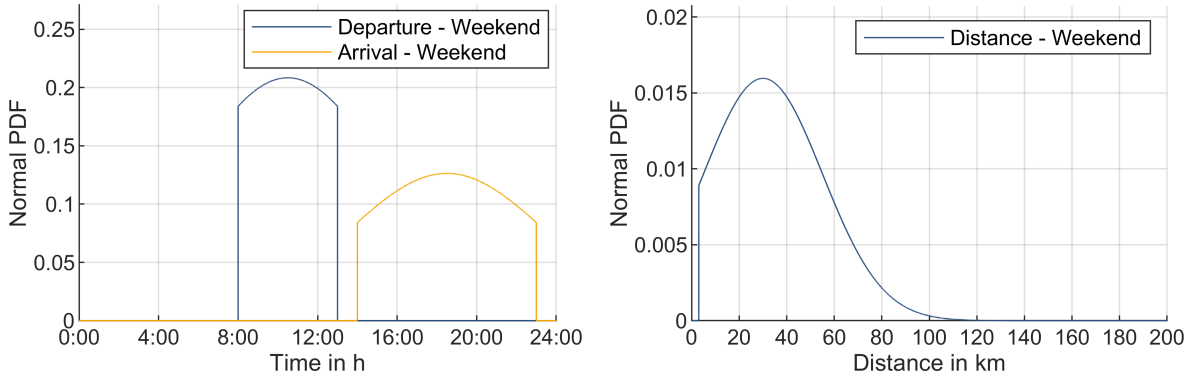

(**a**) (**b**)

Figure 6. Probability density functions (PDFs) of the driving profiles for all mobility profiles on the weekend. (**a**) PDF of the normal distribution used to model the departure and arrival times at home on the weekend (Saturday and Sunday) for all mobility profiles; (**b**) PDF of the normal distribution used to model the driving distance on the weekend (Saturday and Sunday) for all mobility profiles.

Between the departure and arrival at a charging station the vehicle is driving. For the allocated driving distance, we set battery power driving profiles for the EV (DC Battery power while driving). The battery power driving profiles used in this publication are profiles measured in 2017 of a BMW i3 (Motor power: 125 kW, Battery Capacity: 21.6 kWh, Year: 2013).

The consumption (kWh/100km) also changes due to seasonal effects. We measured the consumption of the BMW i3 in 2017. The consumption of the vehicle ranges from 14.0 kWh/100 km in July to 23.9 kWh/100 km in December, due to the lower temperatures in Germany in winter (increased inner resistance of the traction battery, use of heating). The battery power profiles for each trip are therefore set according to the allocated driving distance and the corresponding consumption value for the time of the year.

2.4. Charging Strategies and Scenarios

We simulate different scenarios that differ in the charging strategy used, the mobility profile of the EV, the charging location and the limit setting $SoC_{V2XLimit}$ for the minimal SoC of the EV. The scenario parameters are summarized in Table 3.

Table 3. Summary of scenario parameters.

Charging Strategy	Charging Location	Mobility Profile	$SoC_{V2XLimit}$
Fast	Home (*H*)	Worker	not set
Min-Cal-Aging	Workplace (*W*)	Late Worker	23%
Max-SS	Home & Workplace (*H* + *W*)	2nd Car	
Max-SS-V2H			
FRR			
P_{res}-shave			

We have developed the charging strategies with different objectives in mind. One charging strategy might follow one or more main objectives. The different objectives are the following.

A. Reduction of electricity costs for the owner of the household and the EV
B. Increase of self-consumption of electrical energy generated by the PV systems
C. Increase of self-sufficiency of the household and of the workplace
D. Reduction of calendar battery aging
E. High availability of the EV for mobility
F. Reduction of the power exchanged with the grid by household and workplace

The strategies also depend on different information, such as the departure time of the EV or the measurement of the residual load $P_{Res} = P_{PV,gen} - P_{Load}$. In order to deploy these charging strategies, the energy management system (EMS) controlling the charger has to have this information at its disposal. The charging strategies are explained in Table 4. The objectives, functionalities, and necessary information of the charging strategies are explained in Table 4. An illustration of the power flows and therefore the functionality of the charging strategies for scenarios with home charging only (*H*) is shown in Figure 7.

$SoC_{V2XLimit}$ is set by the driver of the EV as a parameter for the EMS system. V2X stands for the bidirectional use of the EV charger. In bidirectional use, the EV feeds electrical energy to the household or workplace (V2H), or to the grid (V2G). The EMS makes sure that the SoC of the EV does not fall below the limit $SoC_{V2XLimit}$ due to discharging while it is plugged in at the charging station. We simulate scenarios in which this value is not set (EV can be discharged fully) as well as scenarios in which $SoC_{V2XLimit}$ is 23%, which equates to a range of 50 km for a consumption of 15.2 kWh/100 km. The charging location is set to three different settings: "Home Charging" only (*H*), "Workplace Charging" only (*W*) and "Home and Workplace charging" (*H* + *W*).

The different charging strategies are described in Table 4. Following the charging strategy, the charger will set the maximum charging current. The EV will then charge with the charging current set by the charger or a lower charging current due to limitations of the EV.

Table 4. Description of simulated charging strategies.

Charging Strategy	Information
Fast	None
Upon arrival, the EV is charged with the maximum charging power (10 kW) until it is fully charged. This strategy maximizes the availability of the EV for the user (Objective E). See the functionality of the strategy in Figure 7a.	
Min-Cal-Aging	Time of departure of EV
This strategy aims to reduce the average SoC of the EV battery (Objective D). For Li-Ion batteries with an NMC chemistry an elevated SoC leads to accelerated calendar aging [37]. The charge process of the EV is delayed in order to reduce average SoC. The EMS calculates the latest point in time to start charging the EV with maximal power in order to fully charge the EV by the time of departure. See the functionality of the strategy in Figure 7b.	
Max-SS	Time of departure of EV, Residual Load ($P_{Res} = P_{PV,gen} - P_{Load}$)
This strategy charges the EV when positive residual power P_{Res} is available. Then the charging power is set to the value of P_{Res}. As a result the EV is charged with electrical energy generated by the PV system. This strategy aims to increase the self-consumption (SC) and self-sufficiency (SS) of the household (Objectives A, B, and C). If the residual energy is not sufficient to fully charge the EV before departure, the EV is charged with maximum power (10 kW) before departure. See the functionality of the strategy in Figure 7c.	
Max-SS-V2H	Time of departure of EV, residual load, $SoC_{V2XLimit}$
This strategy is an extension of strategy *Max-SS*. In addition to the functionality of *Max-SS*, the EV discharges with negative residual power when load exceeds PV generation. This strategy aims to increase the self-consumption and self-sufficiency of the household using V2H (Objectives A, B, and C). See the functionality of the strategy in Figure 7d.	
FRR	Time of departure of EV, residual load, $SoC_{V2XLimit}$, aFRR request
The EV is integrated into a pool of units that provide positive aFRR. The aggregator of the pool forecasts the power capacity of the pool in order to bid on the aFRR market. For this study we use a time-series of the awarded aFRR participation and the aFRR requests for the time period 30 October 2018–30 July 2019 (9 Months). See Section 2.1 for further details and Figure 3 for a snapshot of the time series. Due to the 4 hour criterion, the power that can be offered by the EV is calculated at the time of plug-in at the charging station. It is calculated as follows, $$P_{aFRR,offered} = (SoC_{t,plug-in} - SoC_{V2XLimit}) \cdot \frac{C_{EV}}{4\,\mathrm{h}},$$ where $SoC_{t,plug-in}$ is the SoC of the EV at the time of plug-in and C_{EV} is the usable capacity of the battery in kWh. The lower limit $SoC_{V2XLimit}$ is the SoC limit for V2X (V2H or V2G) operation to maintain a desired minimal range of the EV at all times. Once the EV is plugged in, the available power for aFRR is calculated and the energy management system waits for a request to provide aFFR. In order to recharge the energy fed to the grid during aFRR operation, an intraday order is placed by the pool aggregator. The intraday order is placed for the time period just before the departure of the EV obeying the restriction on peak charging power. The price to recover the energy on the intraday market is $c_{intraday} + c_{intraday,fees}$. Energy used for driving the vehicle is recharged from the grid with the price $c_{elec,home}$ or $c_{elec.,workplace}$, depending on the charging location, starting at the latest possible point in time before the departure of the EV. This strategy aims to generate additional income from aFRR provision (Objective A). See the functionality of the strategy in Figure 7e.	
P_{res}-shave	Time of departure of EV, residual load, $SoC_{V2XLimit}$, P_{Limit}
The strategy aims to keep the absolute value of the residual load of the household under limit P_{Limit} in order to reduce the power exchanged with the grid (Objective F). In this study $P_{Limit} = 1$ kW. The EV charges with $P_{Res} + P_{Limit}$ when $P_{Res} >= 0$ and discharges to the home with $P_{Res} + P_{Limit}$ when $P_{Res} < -P_{Limit}$. As no forecast algorithms are used, the peak production might not be shaved due to the fact that the EV is already fully charged when it occurs. Moreover, due to the lack of forecast, a peak for the charge of the EV before departure may occur as, starting at the latest possible point in time, the remaining energy is charged with maximum power (10 kW). See the functionality of the strategy in Figure 7f.	

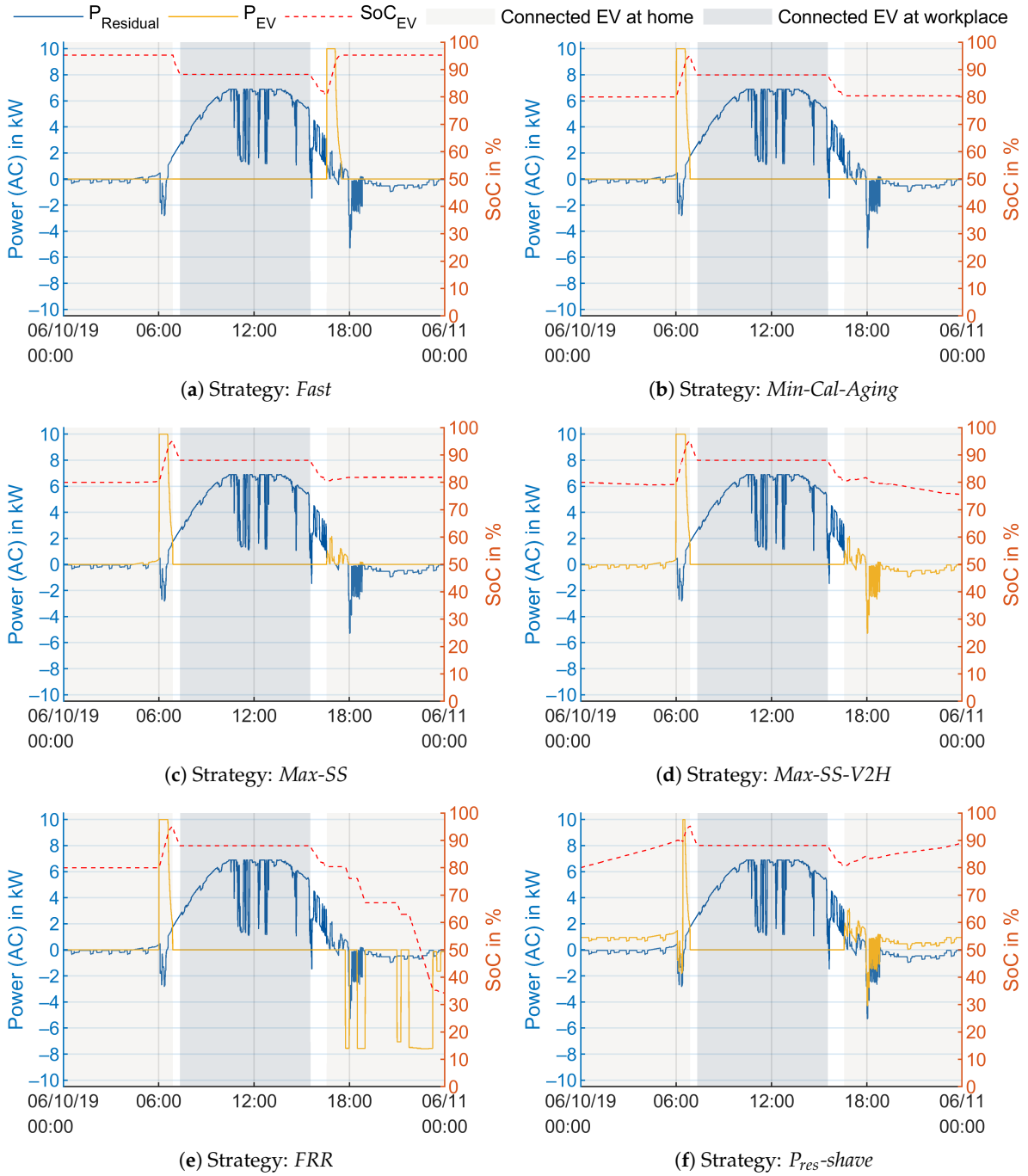

(**a**) Strategy: *Fast*

(**b**) Strategy: *Min-Cal-Aging*

(**c**) Strategy: *Max-SS*

(**d**) Strategy: *Max-SS-V2H*

(**e**) Strategy: *FRR*

(**f**) Strategy: P_{res}*-shave*

Figure 7. Power flows for the household on 10th of June 2019 for mobility profile *Worker* and charging only at home. $P_{Residual} = P_{PV} - P_{inflexibleLoad}$. All power flows on AC side.

Evaluation

We evaluate the impact of the different charging strategies and scenarios using various performance indicators. The Key Performance Indicators (KPI) that evaluate the ecological and economic impact are the direct self-consumption rate (DSC), the self-consumption rate (SC), the self-sufficiency (SS) of the household and the cost for electricity C_e. The DSC rate is the share of electrical energy generated by the PV system that is directly (without storage) consumed in the building where the PV system is mounted (behind-the-meter). The SC rate is the share of electrical energy generated by the PV system that is not fed into the grid but consumed in the building where the PV system is mounted (behind-the-meter).

Storage systems can increase the SC rate but not the DSC rate. The SS rate shows the dependency of the household of the grid connection. It is calculated as

$$SS = 1 - \frac{E_{FromGrid}}{E_{Load/Driving}}, \tag{2}$$

where $E_{FromGrid}$ is the energy drawn from the grid and $E_{Load/Driving}$ is the energy consumption of the inflexible load and the EV. If the household is completely dependent on the grid, the SS rate is 0. For a completely self-sufficient household, the SS rate is 1.

The KPIs regarding the battery stress are the average SoC of the traction battery SoC_{ave} and the equivalent number of full cycles (EFC). Furthermore, we calculate the peak and the 95% and 80% quantiles of the grid exchange power in positive and negative direction to illustrate the impact on the low-voltage grid.

The economic calculations are carried out as follows. The prices are summarized in Table 5. The total electricity cost of the household C_{home} is calculated as

$$\begin{aligned} C_{home} = {} & E_{Home,FromGrid\rightarrow Load/Driving} \cdot c_{electr.,home} \\ & + E_{HomePV\rightarrow Load/EV} \cdot c_{PVgeneration,home} \\ & - E_{HomePV\rightarrow Grid} \cdot (c_{feed-in-tariff,home} - c_{PVgeneration,home}) \end{aligned} \tag{3}$$

$E_{Home,FromGrid\rightarrow Load/Driving}$ is the energy drawn from the grid at the household to cover the inflexible load and the demand of the EV. $E_{HomePV\rightarrow Load/EV}$ is the energy supplied by the PV system to directly cover the inflexible load and the demand of the EV at the household. $E_{HomePV\rightarrow Grid}$ is the energy fed to the grid from the PV system at the household.

The total electricity cost at the workplace $C_{workplace}$ is calculated as

$$\begin{aligned} C_{workplace} = {} & E_{Workplace,FromGrid\rightarrow Driving} \cdot c_{electr.,workplace} \\ & + E_{WorkplacePV\rightarrow EV} \cdot c_{PVgeneration,workplace} \\ & - E_{EV\rightarrow workplace} \cdot c_{feed-in,V2workplace} \end{aligned} \tag{4}$$

$E_{Workplace,FromGrid\rightarrow Driving}$ is the energy drawn from the grid at the workplace to cover the EV demand. $E_{WorkplacePV\rightarrow EV}$ is the energy supplied by the PV system at the workplace to directly cover the EV demand. $E_{EV\rightarrow workplace}$ is the energy supplied by the EV to cover the inflexible load at the workplace. It should be noted that the sale of energy generated by the PV system to the grid is not a factor in Equation (4), as the PV system is not owned by the household owner and EV driver.

The net revenue C_{aFRR}, absolute electricity cost C_e (€) and specific electricity cost c_e (€/kWh) for the owner of the household and EV are calculated as

$$\begin{aligned} C_{aFRR} = {} & E_{FromGrid,Intraday} \cdot \left(c_{intraday} + c_{intraday,fees}\right) \\ & - C_{revenue,aFRR} \end{aligned} \tag{5}$$

$$C_e = C_{home} + C_{workplace} + C_{aFRR}$$

$$c_e = \frac{C_e}{E_{\rightarrow Load,Home} + E_{\rightarrow EV,Driving}} \tag{6}$$

$E_{FromGrid,Intraday}$ is the energy drawn from the grid at the household and workplace which had been ordered on the intraday market. $C_{revenue,aFRR}$ is the revenue in € achieved from the provision of aFRR. $E_{\rightarrow Load,Home}$ is the total energy supplied to cover the inflexible load at the household. $E_{\rightarrow EV,Driving}$ is the total energy supplied at household and workplace to the EV to cover the driving demand.

Table 5. Prices.

Economics	
$c_{electr.,home}$	0.2942 €/kWh (2018)
$c_{PVgeneration,home}$	0.108 €/kWh (2018) [38]
$c_{feed-in-tariff,home}$	0.1220 €/kWh (January–June 2018)
$c_{PVgeneration,workplace}$	0.07 €/kWh (2018) [38]
$c_{intraday,fees}$	12 €/MWh (Grid fees) (based on 5 MWh/5 MW BESS [26])
$c_{intraday}$	see Figure 3
$c_{electr.,workplace}$	0.2222 €/kWh (Electricity price for small businesses with a consumption up to 50 MWh/a) [39])
$c_{feed-in,V2workplace}$	0.2222 €/kWh

3. Results and Discussion

In this section, we evaluate the impact of the charging strategy, the mobility profile, the charging location and the SoC threshold $SoC_{V2XLimit}$ on the direct self-consumption rate (DSC), the self-consumption rate (SC), the self-sufficiency rate (SS), and the electricity cost of the household for the first year (Figures 8–11). It should be noted that the electricity cost for the first year does not correspond to the levelized cost of electricity (LCOE). As the PV system and the EV battery deteriorate with time, the LCOE is higher than the electricity cost for the first year shown here. We also investigate the impact on the power exchange with the grid (Figures 12 and A3–A5) and on stress parameters of battery aging (Figures 13 and A9–A11). In total, we simulated and evaluated 81 scenarios (see Table 3).

In Figures 8–10, the rates for DSC, SC, and SS are plotted together with the electricity cost of the household for one year in € for the scenarios without the limitation $SoC_{V2XLimit}$. The base for the DSC and SC rates is the total energy generated by the PV system of the household, which is 9734 kWh/a. The base for the SS rate depends on the energy provided to cover the load of the household (4274 kWh/a) and the energy provided to charge the EV at the household. With charging strategy *Fast*, the energy (household side of charger) needed to charge the EV is 2874 kWh/a, 2898 kWh/a, and 2013 kWh/a for mobility profiles *Worker*, *Late-Worker* and *2nd Car*, respectively. The energy that has to be provided to the charger varies with the charging strategy used because the charge efficiency depends on the charge power. However, for the calculation of the specific costs c_e (Equation (6)), the value of $E_{\rightarrow EV,Driving}$ is taken from the baseline scenario in order to account for the fact that some charging strategies operate with low charger efficiencies. In Figure 11 the rates and electricity costs of the household are shown for the scenarios with the limitation $SoC_{V2XLimit} >= 23\%$. The limit $SoC_{V2XLimit} >= 23\%$ only has an impact on the results for V2H and V2G strategies. Therefore, only strategies *Max-SS-V2H*, *FRR* and $P_{res} - shave$ are shown in Figure 11. The electricity costs for the household are the costs to power the household (inflexible load) and the mobility (EV consumption). On the x-axis the naming is "Strategy"/"Location". The location variables have the following abbreviations:

H : Charging only at home.
W : Charging only at workplace.
H + W : Charging at home and workplace.

In the following subsections, we discuss the different scenarios and the impact on the DSC, SC, and SS rates, and the electricity costs of the household.

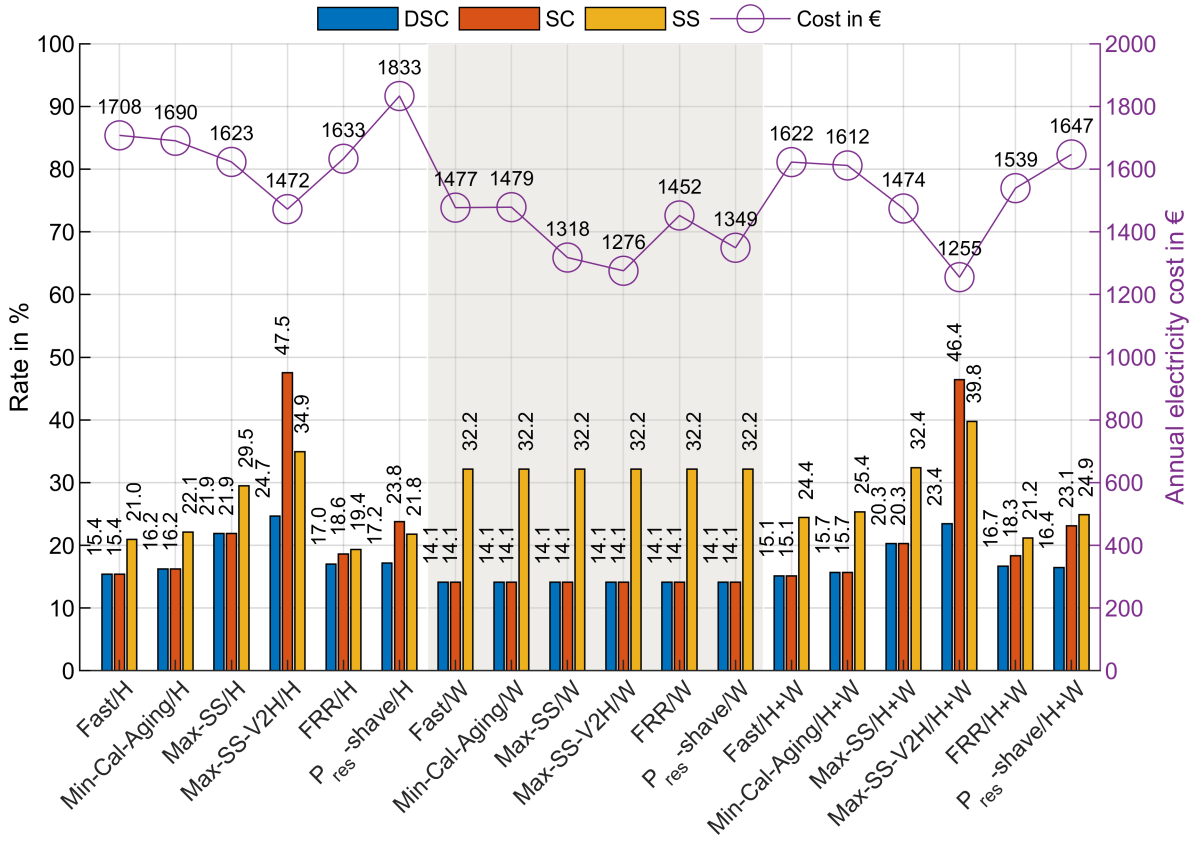

Figure 8. DSC, SC, and SS rates, and electricity cost for mobility profile *Worker* without $SoC_{V2XLimit}$.

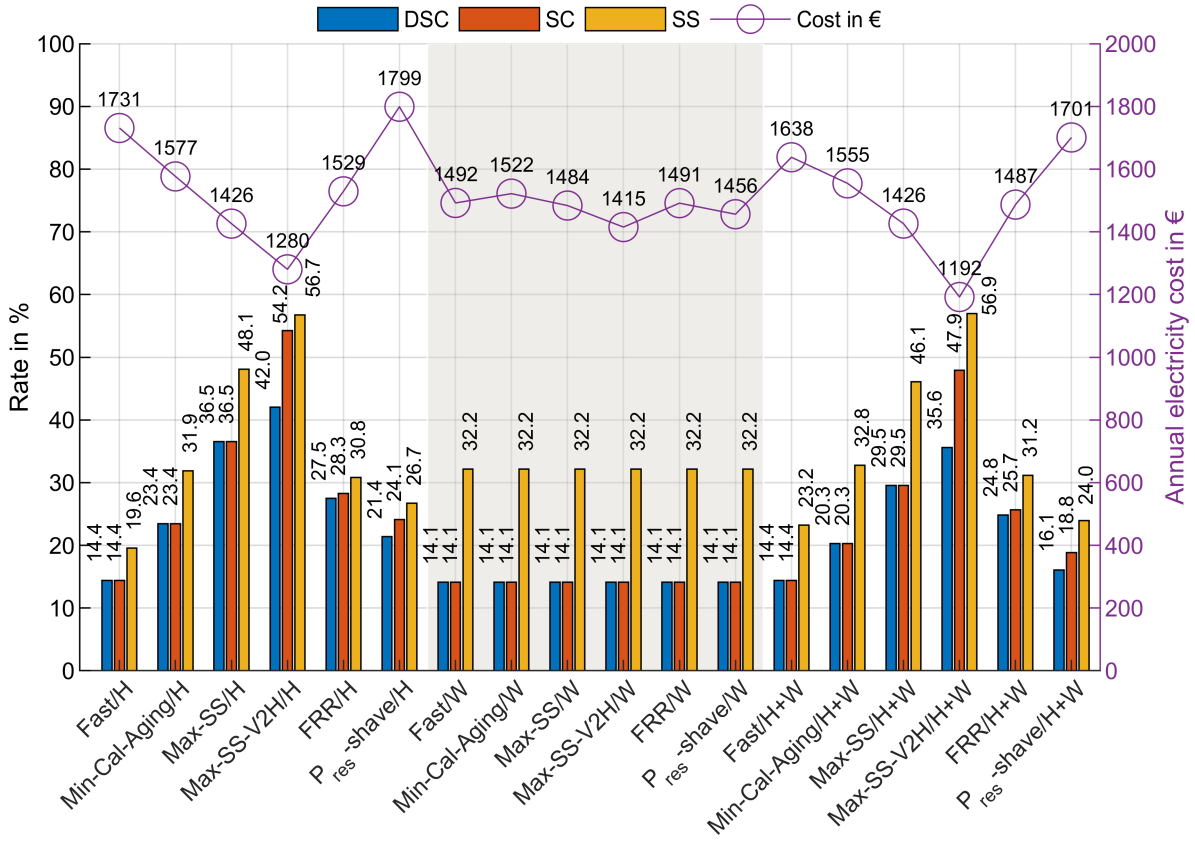

Figure 9. DSC, SC, and SS rates, and electricity cost for mobility profile *Late-Worker* without $SoC_{V2XLimit}$.

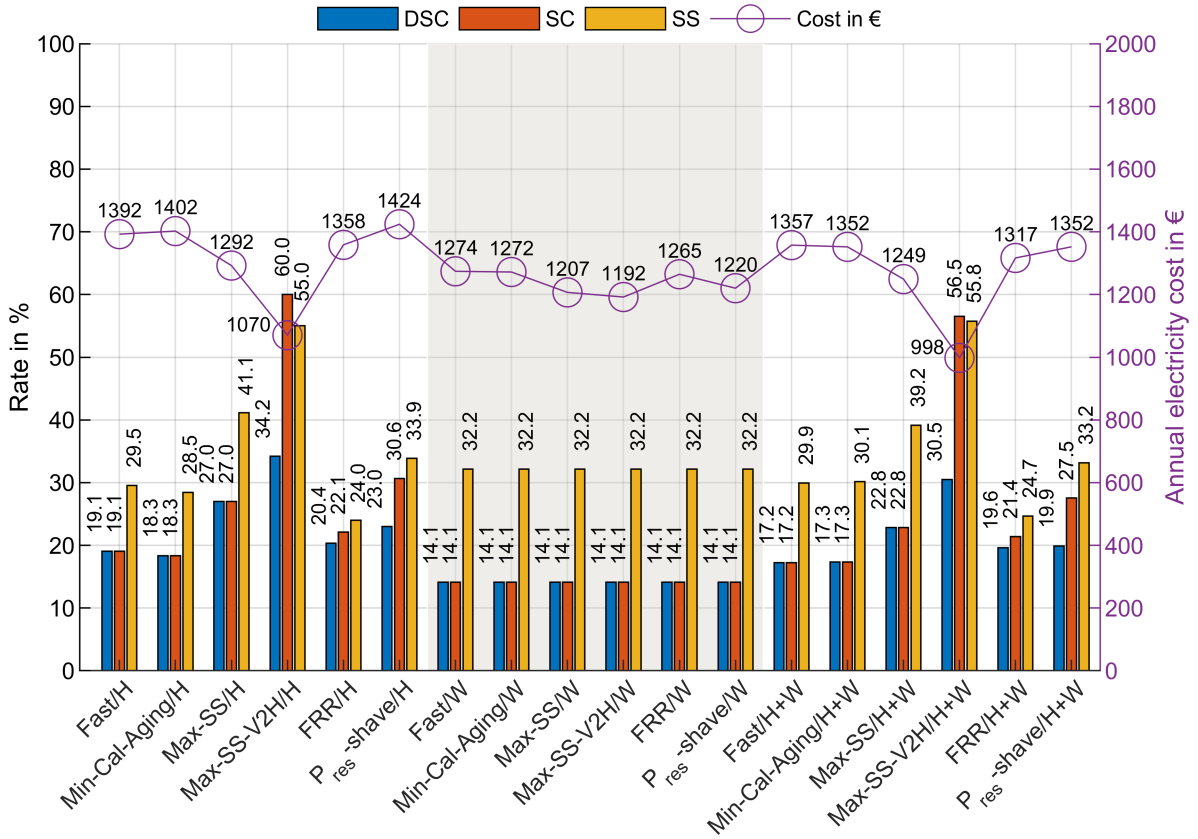

Figure 10. DSC, SC, and SS rates, and electricity cost for mobility profile *2nd Car* without $SoC_{V2XLimit}$.

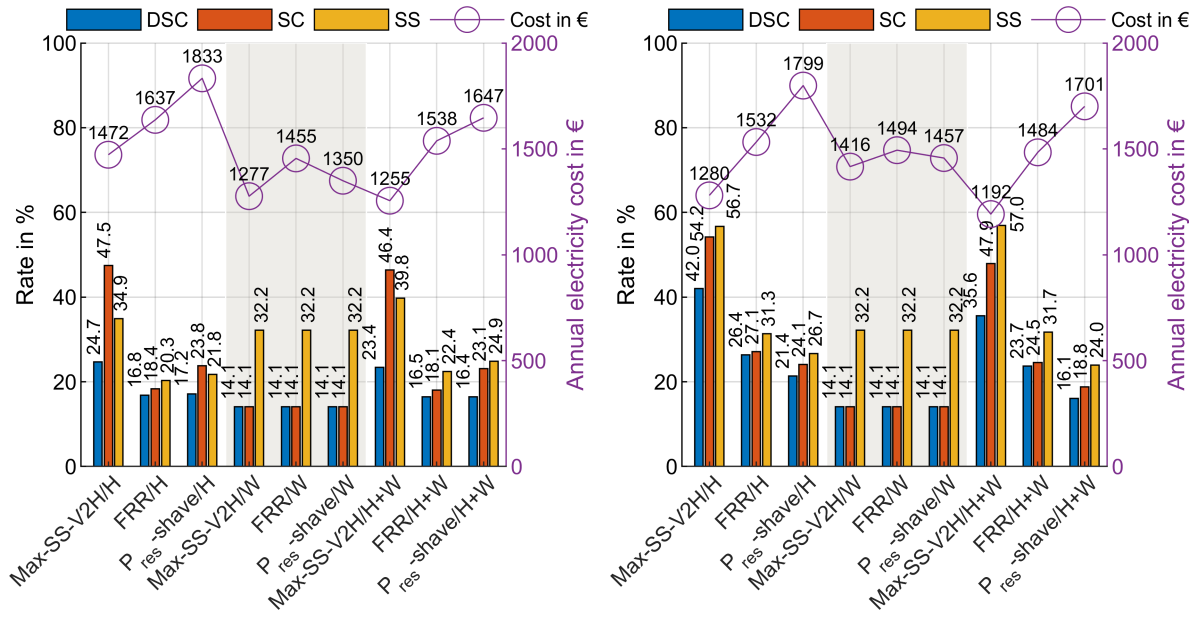

(**a**) Mobility profile *Worker* (**b**) Mobility profile *Late Worker*

Figure 11. *Cont.*

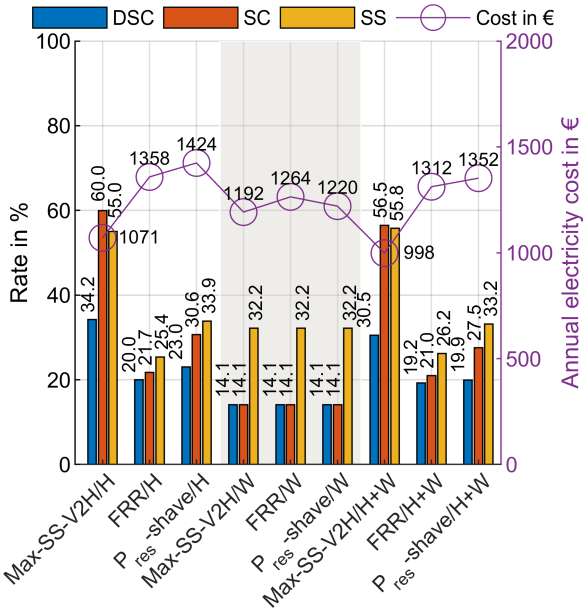

(**c**) Mobility profile *2nd Car*

Figure 11. DSC, SC, and SS rates, and electricity cost for scenarios with $SoC_{V2XLimit} = 23\%$.

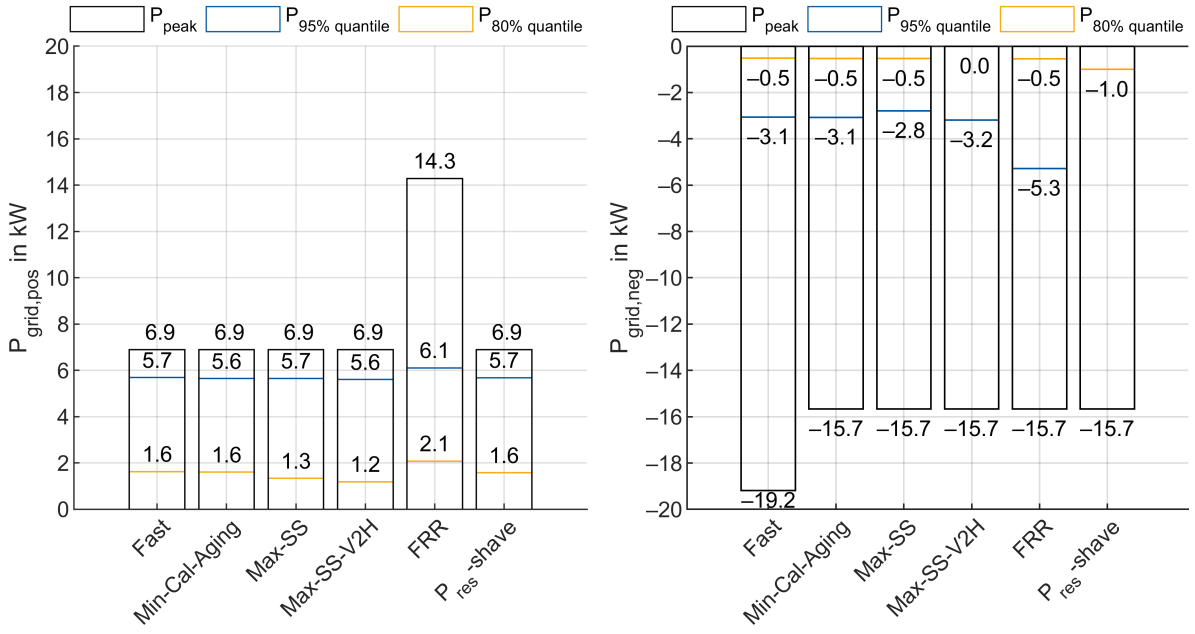

(**a**) (**b**)

Figure 12. Power exchange of the household with the grid for the home charging scenario *H* and mobility profile *Worker* without $SoC_{V2XLimit}$. (**a**) Positive power exchange (Household → Grid). (**b**) Negative power exchange (Grid → Household).

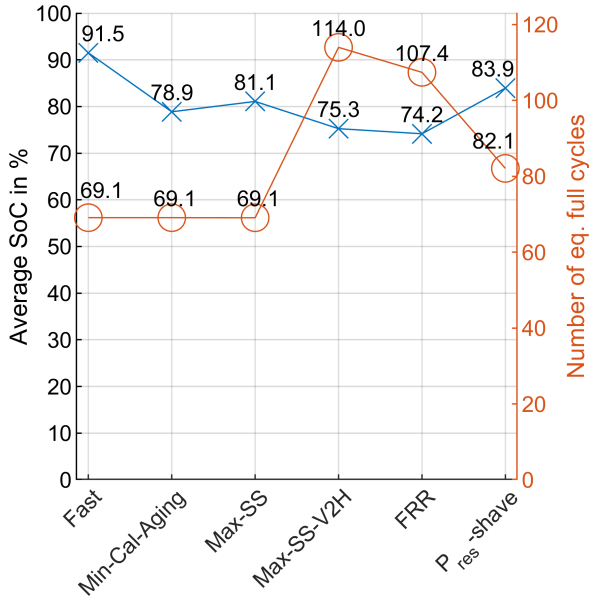

Figure 13. Average SoC and number of equivalent full cycles for scenario home charging *H*, mobility profile *Worker* and without $SoC_{V2XLimit}$.

3.1. Workplace Charging Scenarios

The results for the workplace scenarios (*W*) can be easily spotted in the figures as they are marked with a grey area in the background. For the *W* scenarios, the DSC, SC, and SS rates stay constant for all charging strategies and all mobility profiles. As the EV does not charge at the household in this scenario, the charging strategy and the driving profile have no impact on the electricity consumption of the household. In this case, 14.1% (1373 kWh) of electrical energy generated by the PV system is consumed directly in the household (DSC). As no energy storage systems are integrated in the household, the SC rate equals the DSC rate. The SS rate is 32.2% for the household. The electricity cost is affected by the charging strategy and the mobility profile as the workplace also possesses a PV system. The share of PV energy used to charge the EV impacts the electricity cost. The electricity cost varies between the mobility profiles as the departure and arrival times and the driving distances differ between them. As expected, the mobility profile *2nd Car* (Figure 10) has the lowest electricity costs because the EV drives 4512 km (30%) less than in profile *Worker* and 4713 km (32%) less than in profile *Late-Worker*. Strategies *Fast* and *Min-Cal-Aging* exhibit the highest cost for all mobility profiles in the W scenarios. Strategy *Max-SS-V2H* yields the lowest cost for all mobility profiles and without $SoC_{V2XLimit}$.

3.2. Home Charging Scenarios

In the home charging scenarios (*H*), the charging strategy of the EV has an impact on the DSC, SC, and SS rates, and the electricity cost of the household. In comparison to the workplace scenarios, the DSC and SC rates have increased. For the baseline strategy *Fast*, the introduction of the charging station for the EV at the household reduces the SS rate of the household as the EV charges predominantly with energy provided from the grid. This is also true for mobility profile *Worker*, as the EV is seldom connected at hours of high PV energy generation. Mobility profiles *Late-Worker* and *2nd Car* show increased SS rates compared to the *W* scenario with the unidirectional strategy *Max-SS*. The bidirectional strategy *Max-SS-V2H* leads to the largest SC and SS rates across all mobility profiles. This also manifests itself in the lowest electricity costs of all strategies. The SS rate reaches up to 56.7% (5276 kWh) for profile *Late-Worker* and the *Max-SS-V2H* strategy without $SoC_{V2XLimit}$. The lowest electricity costs are reached with 1070 €/a (17 €ct/kWh) for profile *2nd Car* and without $SoC_{V2XLimit}$.

3.3. Home and Workplace Charging Scenarios

The home and workplace charging scenarios $H + W$ reach lower DSC, SC, and SS rates than the home charging scenario (H), as the EV also charges at the workplace. Due to the favorable prices at the workplace ($c_{electr.,workplace} < c_{electr.,home}$, $c_{PV generation,workplace} < c_{PV generation,home}$ and $c_{feed-in,V2workplace} > c_{feed-in-tariff,home}$), the electricity costs of the $H + W$ scenarios are lower than for the H scenarios. The lowest electricity cost is reached with 998 €/a (15.9 €ct/kWh) for profile *2nd Car* and strategy "Max-SS-V2H". This is also the global minimum for the electricity cost for all scenarios. In the $H + W$ scenario electrical energy generated at the household from PV can be sold at the workplace. That explains the very low costs of V2X strategies for the $H + W$ scenarios.

3.4. Fast Strategy

We set the *Fast* charging strategy as the baseline strategy in this publication. Overall, the *Fast* strategy leads to the second highest electricity cost and low DSC, SC, and SS rates. The electricity cost is in the range of 1392 €/a (22.1 €ct/kWh) to 1731 €/a (24.1 €ct/kWh) for H scenarios, 1274 €/a (20.3 €ct/kWh) to 1492 €/a (20.8 €ct/kWh) for W scenarios, and 1357 €/a (21.6 €ct/kWh) to 1638 €/a (22.8 €ct/kWh) for $H + W$ scenarios.

3.5. Min-Cal-Aging Strategy

The strategy *Min-Cal-Aging* shifts the charging start from the arrival time to the latest time possible to still be able to fully charge the car before departure. The difference in electricity cost therefore depends on the share of PV energy at the new charging time just in time before departure. For mobility profiles *Worker* and "Late-Worker" in the H and $H + W$ scenarios, the shift is beneficial as the SC and SS rates increase and the costs drop. The costs increase or stay constant for all scenarios with mobility profile *2nd Car* and for W scenarios. In the mobility profile *2nd Car*, the EV departs in the morning and arrives at the household at noon/afternoon during a workday. A shift of the home charging process towards the morning hours therefore increases costs for this mobility profile, as less electrical energy generated from the PV system is used to charge the EV.

3.6. Max-SS Strategy

As intended, the *Max-SS* charging strategy leads to increased SC and SS rates and decreased electricity costs for all scenarios. With this unidirectional strategy, the self-sufficiency (SS) of the household increases by 8.5–28.5% for the H scenario and by 8–22.9% for the $H + W$ scenarios compared to the baseline strategy *Fast*. The electricity costs for the year of simulation were reduced by 85 €/a (4.9%) − 305 €/a (17.6%) for the H scenarios, by 8 €/a (0.5%) − 159 €/a (10.7%) for the W scenarios and by 108 €/a (8.0%) − 212 €/a (12.9%) for the $H + W$ scenarios compared to the baseline strategy *Fast*. Strategy *Max-SS* has a very high impact on the *Late-Worker* and H and $H + W$ scenarios, as the positive residual load during the morning hours until noon can be used to charge the EV on workdays.

3.7. Max-SS-V2H Strategy

Strategy *Max-SS-V2H* yields the highest SC and SS rates and lowest electricity costs for all mobility profiles and charging locations. With this charging strategy, the EV shifts PV energy to cover inflexible household or workplace load at a later time. This results in greatly increased SC and SS rates. The SC rate reaches its maximum with 60% for profile *2nd Car* and home charging (H) and the SS rate reaches its maximum with 56.9% for profile *Late Worker* and home and workplace charging ($H + W$) . For home charging (H), the electricity costs decrease 236 €/a (13.8%) − 451 €/a (26.1%) with the *Max-SS-V2H* strategy compared to the baseline strategy *Fast*. For workplace charging (W), the electricity costs decrease 77 €/a (5.2%) − 201 €/a (13.6%). In the W scenario, electrical energy generated from the PV system can be stored and subsequently sold back with a high profit margin. The largest decrease in electricity costs is reached with the scenario with combined home and workplace

charging ($H + W$) with a decrease of 367 €/a (22.6%) − 446 €/a (27.2%). The scenario $H + W$ has the lowest cost with 1255 €/a (17.6 €ct/kWh) for profile *Worker*, 1192 €/a (16.6 €ct/kWh) for profile *Late Worker* and 998 €/a (15.9 €ct/kWh) for profile *2nd Car*. The impact of the limit $SoC_{V2XLimit} >= 23\%$ for strategy *Max-SS-V2H* is negligible for all scenarios (see Figure 11). The reduction in availability of the EV, as it might discharge to very low SoC values during the V2X operation, is not outweighed by cost savings. Therefore, the limitation of $SoC_{V2XLimit} >= 23\%$ during V2X operation may be a sensible option to ensure that the EV offers a reasonable driving distance at all times.

3.8. FRR Strategy

Strategy *FRR* is an extension of *Max-Cal-Aging*. As the EV is discharged when it provides positive aFRR, the subsequent charge uses more electrical energy generated by the PV system. This is visible in Figures 8–10 with the increase of the DSC and SC rates in comparison to the *Min-Cal-Aging* strategy. In contrast, the SS rates are reduced as the electricity demand of the household is increased greatly as energy provided for aFRR has to be recovered from the grid. The costs for intraday orders and grid fees are lower than the revenue from aFRR provision. This yields a positive net return for all scenarios as is illustrated in Figure 14a,b.

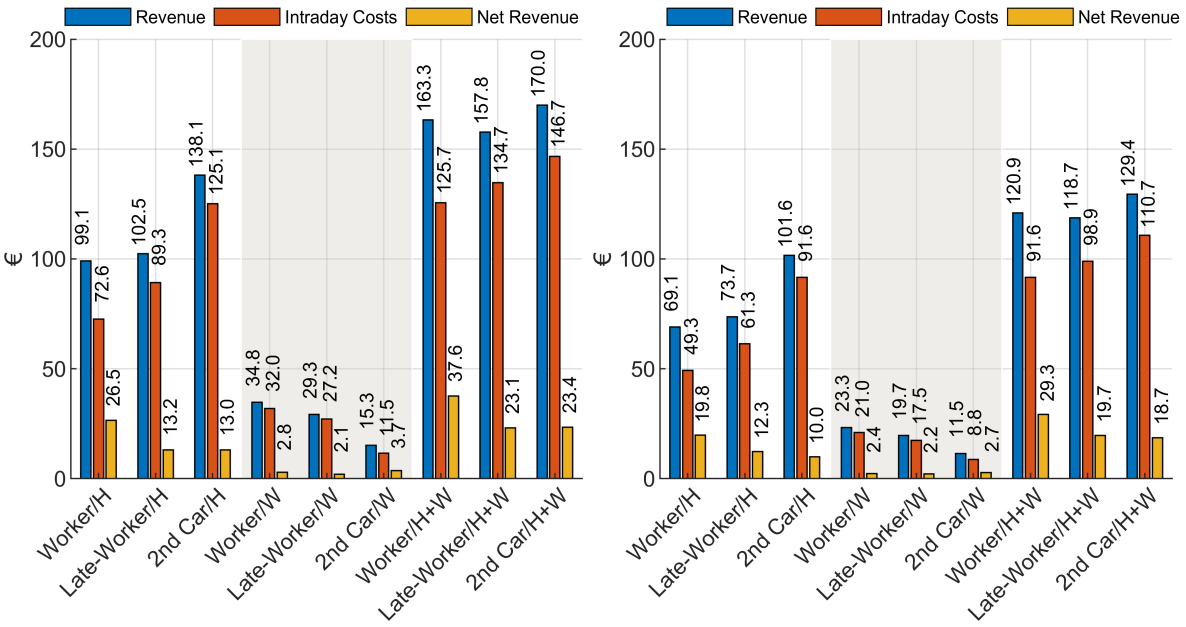

(**a**) Without $SoC_{V2XLimit}$ (**b**) $SoC_{V2XLimit} = 23\%$

Figure 14. Revenue of aFRR provision, Intraday costs, and Net Revenue for *FRR* strategy.

For scenarios without $SoC_{V2XLimit}$ (Figure 14a), the revenue for aFRR provision ranges from 15.3 € ("2nd Car/W") to 170 € ("2nd Car/H+W") for the time period 30.10.2018–31.7.2019. The net revenue is in the range of 2.1 € ("Late-Worker/W") and 37.6 € ("Worker/H+W"). With the limit $SoC_{V2XLimit} >= 23\%$, revenues and net revenues are significantly reduced. The highest revenue for scenario "2nd Car/H+W" is reduced by 24% and the net revenue of "Worker/H+W" is reduced by 20%. Overall, strategy *FRR* leads to a significant reduction in electricity costs for all scenarios in comparison to the *Max-Cal-Aging* and *Fast* scenario but not to the same extent as the *Max-SS-V2H* strategy. For further studies a combination of the *Max-SS-V2H* strategy and the *FRR* strategy could yield an additional cost benefit. Additionally, negative aFRR could be provided by the EV.

3.9. P_{res} − *shave* Strategy and the Power Exchanged with the Grid

Strategy P_{res} − *shave* yields mixed results for rates and electricity costs as its aim is not only self-consumption and self sufficiency maximization, but also the reduction of the peak power exchanged with the grid. Especially in the scenarios with H charging, the use of strategy P_{res} − *shave*

leads to a significant increase of electricity costs by 32 €/a (2.3%)–125 €/a (7.3%). In this case, the use of this strategy would have to be incentivized by the grid operator.

In Figure 12 the power exchanged with the grid for the home charging scenarios without $SoC_{V2XLimit}$ and mobility profile *Worker* is shown. These scenarios show the largest values for the power exchanged with the grid. In Figure 12a the positive peak power, 95% quantile and 80% quantile are shown. The *FRR* strategy yields the highest power exchange as expected. All other strategies yield a peak of 6.9 kW, which is the peak output of the PV inverter minus the baseload of the household. Strategy *Max-SS-V2H* yields reduced power quantile values, yet strategy $P_{res} - shave$ does not yield a significant reduction as the EV is not present regularly during hours of PV production. In Figure 12b the negative peak power, 95% quantile and 80% quantile are shown. Strategy *FRR* exhibits the largest absolute value for the 95% quantile and $P_{res} - shave$ exhibits the lowest. Strategy $P_{res} - shave$ shows its functionality with a reduced 95% quantile, but it does not reduce the peak power drawn from the grid as it does not operate with a forecast strategy. Overall, a forecast strategy should be included to achieve further reduction of the power exchanged with the grid. Further evaluations of the negative power exchange are found in Figures A3–A5, and of the positive power exchange in Figures A6–A8.

3.9.1. Average SoC and Number of Equivalent Full Cycles

In Figure 13, the average SoC and the number of equivalent full cycles of the traction battery are shown for the scenario of home charging, mobility profile *Worker* and without $SoC_{V2XLimit}$. The results for the other scenarios are shown in Figures A9–A11. The average SoC of a Li-Ion battery affects its calendar aging as a high SoC leads to accelerated calendar aging. Figure 13 shows that the average SoC of the battery during the simulation time of one year is quite high for all charging strategies. In order to reduce the degradation of the battery, manufacturers limit the usable SoC range of the battery. In this case, the maximum SoC that can be reached is 95.3%. This limit is set by the BMS of the EV. For strategy *Fast*, the average SoC is 91.5%, which is the highest of all charging strategies. The strategy *Min-Cal-Aging* shows the lowest average SoC of the unidirectional charging strategies with 78.9%. However, the EV battery is not oversized, as the EV sometimes uses its full range on a weekend trip. In order to further reduce the average SoC, a maximum SoC Limit could be introduced for days on which only low driving distances are expected.

The V2X charging strategies *Max-SS-V2H* and *FRR* yield lower average SoCs as the battery is discharged when it is plugged in. Strategy *FRR* exhibits the lowest average SoC with 74.2% for the mobility profile *Worker* and the scenario home charging *H*. The reduction of battery aging by a lower average SoC can be assessed with battery aging models. With the battery aging model of a Li-Ion NMC high-energy cell parametrized in [37] we can estimate the reduction of battery aging due to a lower average SoC as the EV in this study is also equipped with Li-Ion NMC high-energy cells. The lifetime of a battery cell stored at 74.2% SoC is 43% higher than of a battery cell stored at 91.5% SoC, where the cell temperature is 20°C in both cases. It should be noted that the dependence of calendaric battery aging on the SoC of the battery cell is not linear.

The V2X operation, however, leads to an increased number of equivalent full cycles, which leads to increased cycle aging [37]. For the scenario home charging *H* and mobility profile *Worker* the strategy *Max-SS-V2H* leads to maximum value of 114 EFC.

4. Conclusions

We investigated smart charging strategies and the provision of positive automatic Frequency Restoration Reserve (aFRR) with an electric vehicle (EV, 38 kWh) in a prosumer household with a photovoltaic (PV) system (10 kW_p) for the first year of operation. The simulated time frame was 30 October 2018–30 October 2019. We compared our results to a baseline scenario with the charging strategy *Fast*, which charges the EV with maximum power (10 kW) once the EV is plugged in. We investigated scenarios with home charging only (*H*), workplace charging only (*W*) and combined home

and workplace charging (*H* + *W*) for three mobility profiles *Worker*, *Late-Worker*, and *2nd Car*. The three different mobility profiles influence the results for DSC, SC, and SS rates and the electricity costs.

If the EV is only charged at the household and the charger is unidirectional, a charging strategy that aims to maximize the self-sufficiency of the prosumer household (*Max-SS*, Maximization of self-sufficiency of a prosumer household), reaches a self-sufficiency rate of the household of 29.5–48.1% depending on the mobility profile. This corresponds to an electricity cost reduction of 85 €/a (4.9%)–305 €/a (17.6%). We found that strategies *Max-SS*, *Max-SS-V2H* (Maximization of self-sufficiency of a prosumer household using a bidirectional charger), and *FRR* (Provision of positive aFRR) yield beneficial results for all mobility profiles when applied.

With the use of a bidirectional charger and charging strategy *Max-SS-V2H*, a self-sufficiency rate of 34.9–56.7% is reached for home charging (*H*) depending on the mobility profile. This equates to an electricity cost reduction of 236 €/a (13.8%)–451 €/a (26.1%). The result illustrates high potential of smart charging strategies to reduce costs and the emission of GHG. For the unidirectional strategy *Max-SS*, only an EMS and the input of the desired departure time of the EV is needed to make use of this potential. For the bidirectional strategy *Max-SS-V2H*, an additional investment in a bidirectional charger is necessary. Furthermore, the user of the EV has to evaluate, if the cost savings outweigh the operational restrictions (EV is not always fully charged). In order to consider this factor, we investigated the addition of a lower SoC limit $SoC_{V2XLimit} = 23\%$ (50 km range) for the V2X operation. The limit does not have a significant impact on the cost reductions and is therefore a sensible option to ensure that the EV is operational at all times. Another cost factor that has to be compared for the different charging strategies is the impact on battery aging. All strategies reduce the average SoC of the battery, compared to the baseline strategy, which yields a favourable effect in terms of calendar battery aging [37]. While the unidirectional strategies exhibit the same number of equivalent full cycles (EFC), the bidirectional strategies increase the number by up to 40%. In the scenario with home charging *H*, mobility profile *Worker* and the strategy *Max-SS-V2H*, the number of equivalent full cycles is 114. Li-Ion NMC high-energy cells show a cycle lifetime of over 2200 cycles for 10% depth-of-discharge [37]. As the lifetime of a vehicle is in the range of 15 to 20 years the increase of the equivalent full cycles does not have a significant impact on battery aging. However, further investigations have to be done to quantify the impact of the smart charging strategies on battery aging.

We also investigated the impact of charging the EV at the workplace where a PV system is also installed. In this study, we assumed that the EV owner can purchase/sell electricity from/to the workplace. As the electricity price at the workplace and the generation cost for PV electricity is lower than at the household, it is a great incentive for the worker to purchase an EV, as this further reduces his/her electricity costs.

The largest cost reduction is achieved, if the EV is charged at home and at the workplace. In this scenario, the EV is charged predominantly with PV power. In addition, as the workplace pays for energy from V2Workplace operation, the EV shifts PV energy with a positive net revenue. This adds greatly to the reduced electricity costs in these scenarios. The electricity cost for the EV owner is reduced by 359 €/a (26.4%)–446 €/a (27.2%) to a specific electricity cost of the household of 15.9 €ct/kWh–17.6 €ct/kWh using strategy *Max-SS-V2H* for the first year of operation and all mobility profiles.

The provision of positive aFRR from 30 October 2018–31 July 2019 yielded a positive net return for all scenarios without considering additional investment cost for a control unit. However, the net return was low with a value of 2.1 € to 37.6 €. The electricity costs for the scenarios with the aFRR strategy also exceeded the costs for those with the Max-SS-V2H strategy. For participation on the aFRR market, a control unit costing between 299 € [40] and 1000 € would be needed [41] , which would lead to annual costs of 20 € to 67 € for a depreciation period of 15 years.

In conclusion, the unidirectional strategy *Max-SS* and bidirectional strategy *Max-SS-V2H* provide significant reduction of electricity costs GHG emission. Strategy *Max-SS-V2H* offers the greatest reduction, surpassing also the provision of positive aFRR for prosumer households. The provision of

positive aFRR could only be profitable if the current costs of the necessary control unit would decrease dramatically. Smart charging strategies lead to reduced average SoCs of the traction battery which reduces calendar aging. The impact of V2X strategies on cycle aging has to be further investigated. In addition to the provision of positive aFRR the EVs could also provide negative aFRR which could lead to added electricity cost reductions.

Author Contributions: F.R., I.S., and M.M. conceptualized the study and wrote the manuscript. R.V.-R., J.G., and I.S. supported the modification and improvement of the paper. D.U.S. coordinated the research that led to the results presented in this paper.developed the methodology. All authors contributed to structuring the study. All authors have read and agreed to the published version of the manuscript.

Funding: The project upon which this publication is based was funded by the German Federal Ministry of Transport and Digital Infrastructure under project number 16SBS001C.

Conflicts of Interest: The authors declare no conflicts of interest.

Abbreviations

The following abbreviations are used in this manuscript:

aFRR	Automatic Frequency Restoration Reserves
BMS	Battery Management System
BRP	Balance Responsible Party
DSC	Direct Self-Consumption
EEG	Renewable Energy Sources Act
EFC	Equivalent Full Cycle
EMS	Energy Management System
EV	Electric Vehicle
FCR	Frequency Containment Reserve
GHG	Greenhouse Gas
KPI	Key Performance Indicator
LFC	Load Frequency Control
mFRR	Manual Frequency Restoration Reserve
PDF	Probability Density Function
PV	Photovoltaic
RR	Replacement Reserve
SC	Self-Consumption
SoC	State of Charge
SS	Self-Sufficiency
TSO	Transmission System Operator
V2X	Vehicle-to-X
V2G	Vehicle-to-Grid
V2H	Vehicle-to-Home

Appendix A.

Appendix A.1. Mobility Profiles 2 and 3

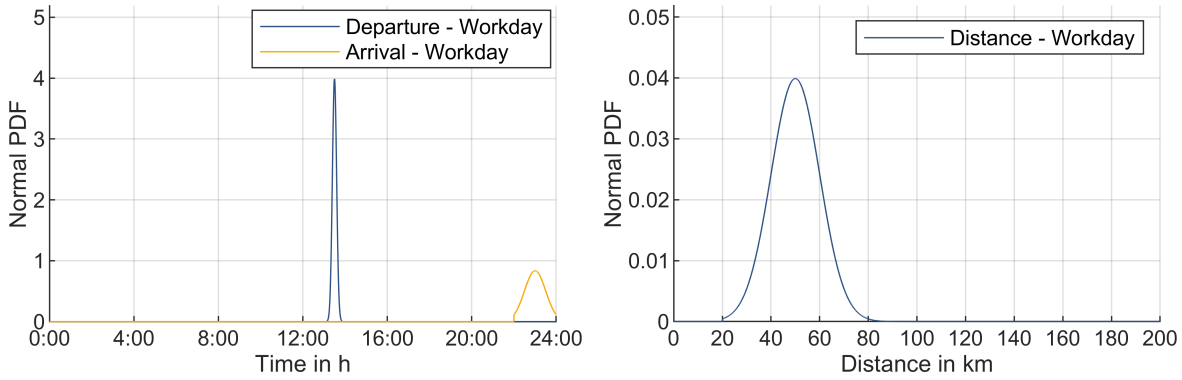

Figure A1. Probability distribution functions (PDFs) of the driving profiles for mobility profile *Late Worker* on a workday. (**a**) PDF of the normal distribution used to model the departure and arrival times at home on a workday (Monday–Friday) for mobility profile *Late Worker*; (**b**) PDF of the normal distribution used to model the driving distance on a workday (Monday–Friday) for mobility profile *Late Worker*.

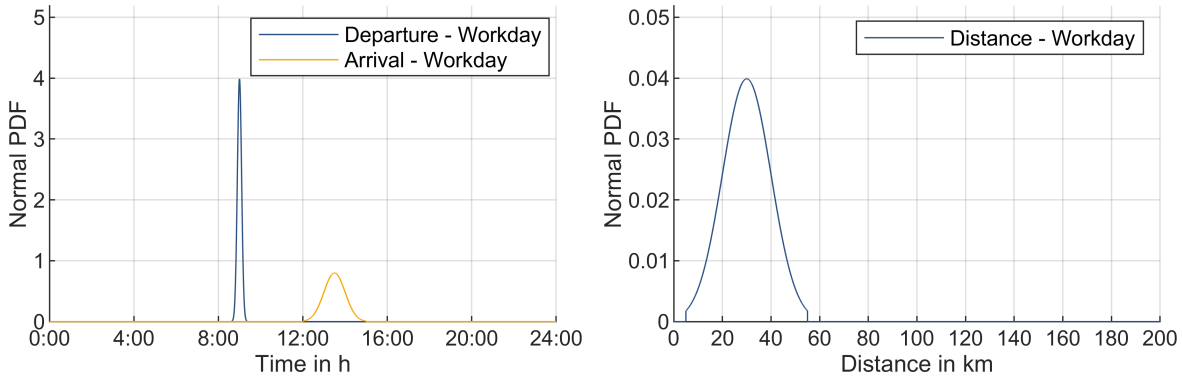

Figure A2. Probability distribution functions (PDFs) of the driving profiles for mobility profile *2nd Car* on a workday. (**a**) PDF of the normal distribution used to model the departure and arrival times at home on a workday (Monday–Friday) for mobility profile *2nd Car*; (**b**) PDF of the normal distribution used to model the driving distance on a workday (Monday–Friday) for mobility profile *2nd Car*.

Appendix A.2. Grid Power Exchange and Battery Stress

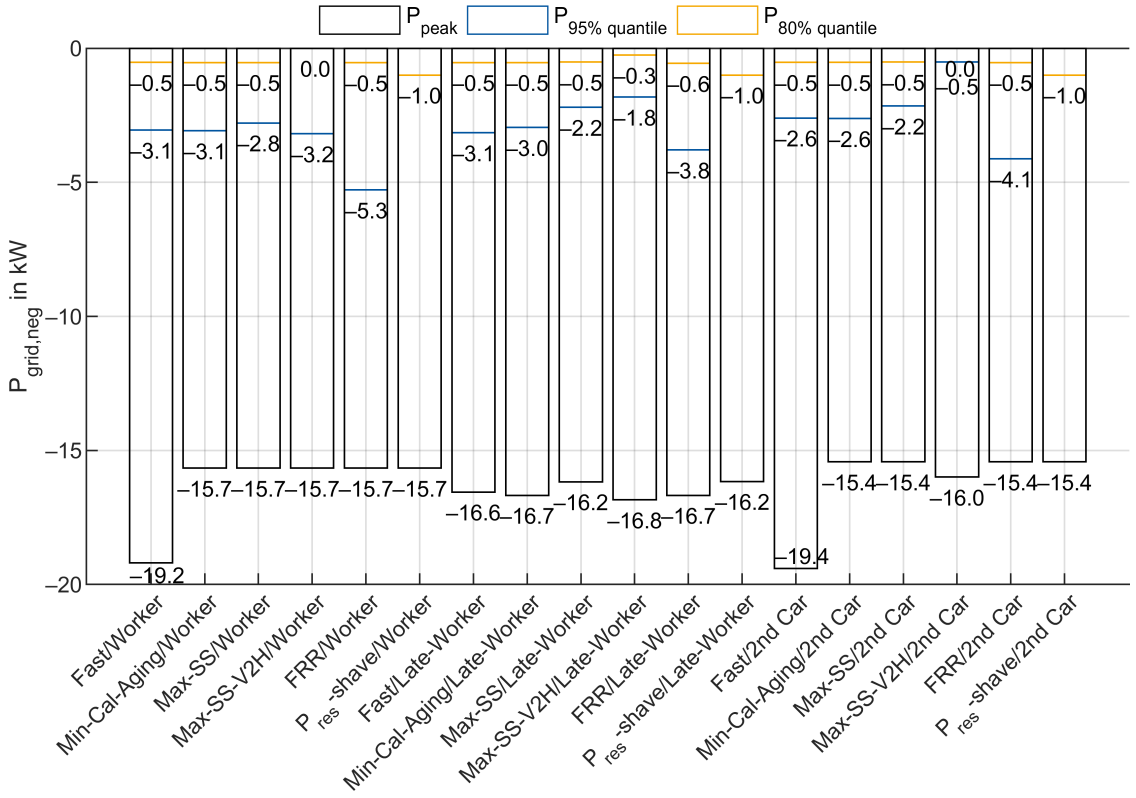

Figure A3. Negative power exchange of the household with the grid for home charging scenario *H* without $SoC_{V2XLimit}$.

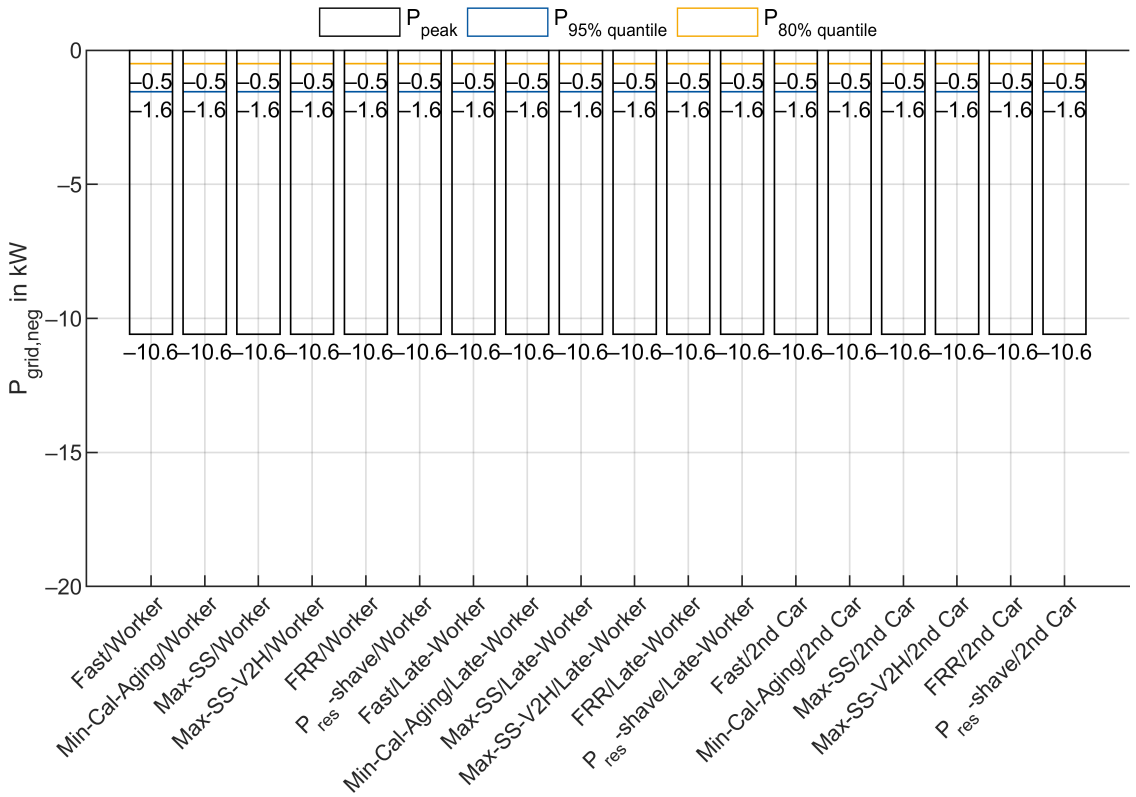

Figure A4. Negative power exchange of the household with the grid for workplace charging scenario *W* without $SoC_{V2XLimit}$.

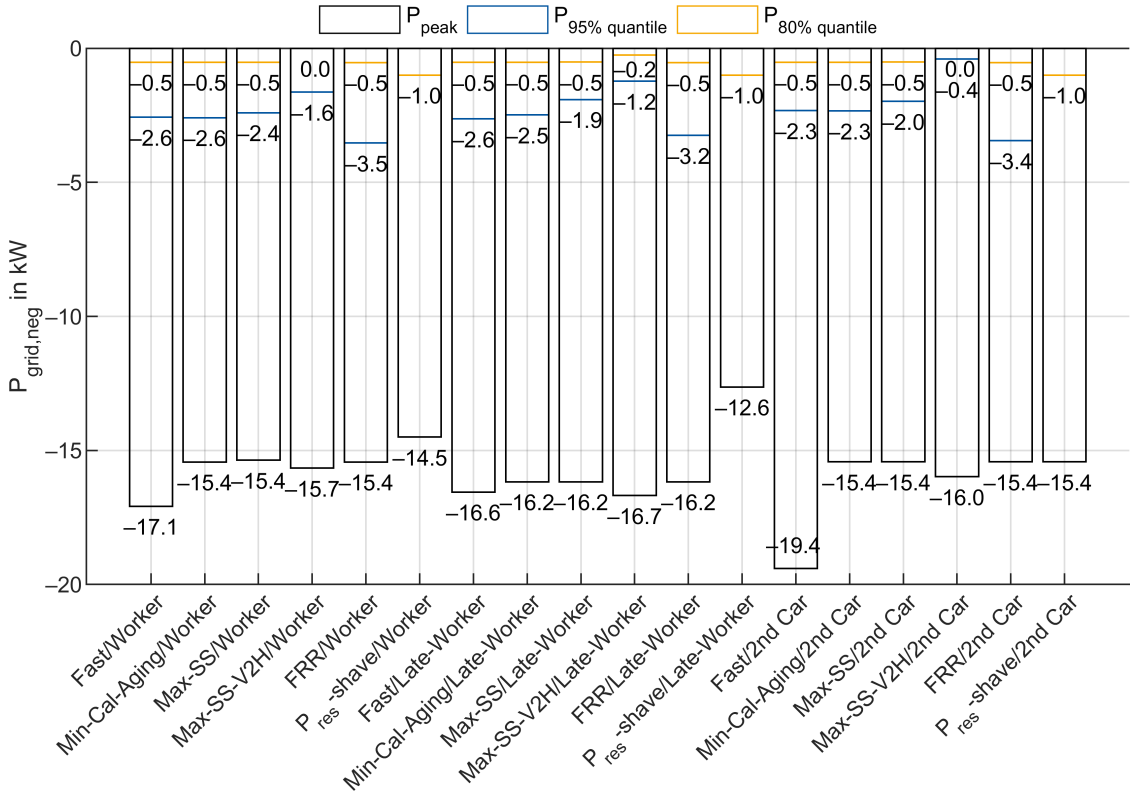

Figure A5. Negative power exchange of the household with the grid for workplace and home charging scenario $H + W$ without $SoC_{V2XLimit}$.

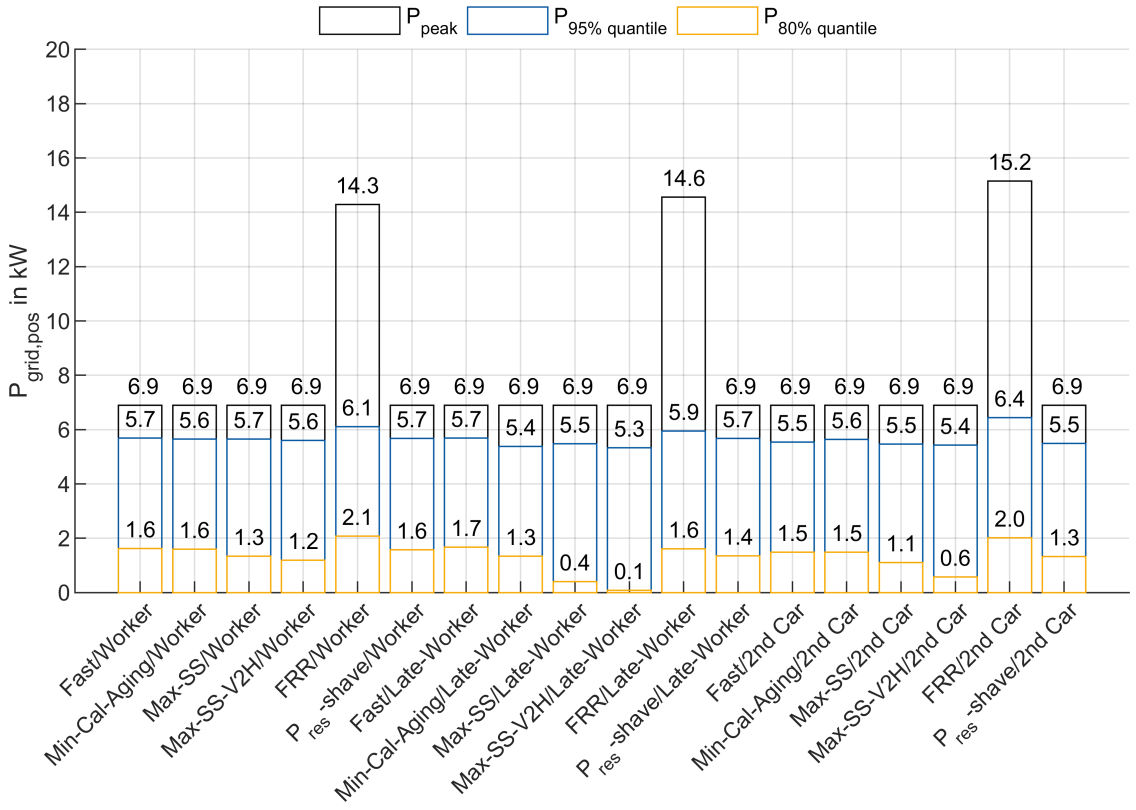

Figure A6. Positive power exchange of the household with the grid for home charging scenario H without $SoC_{V2XLimit}$.

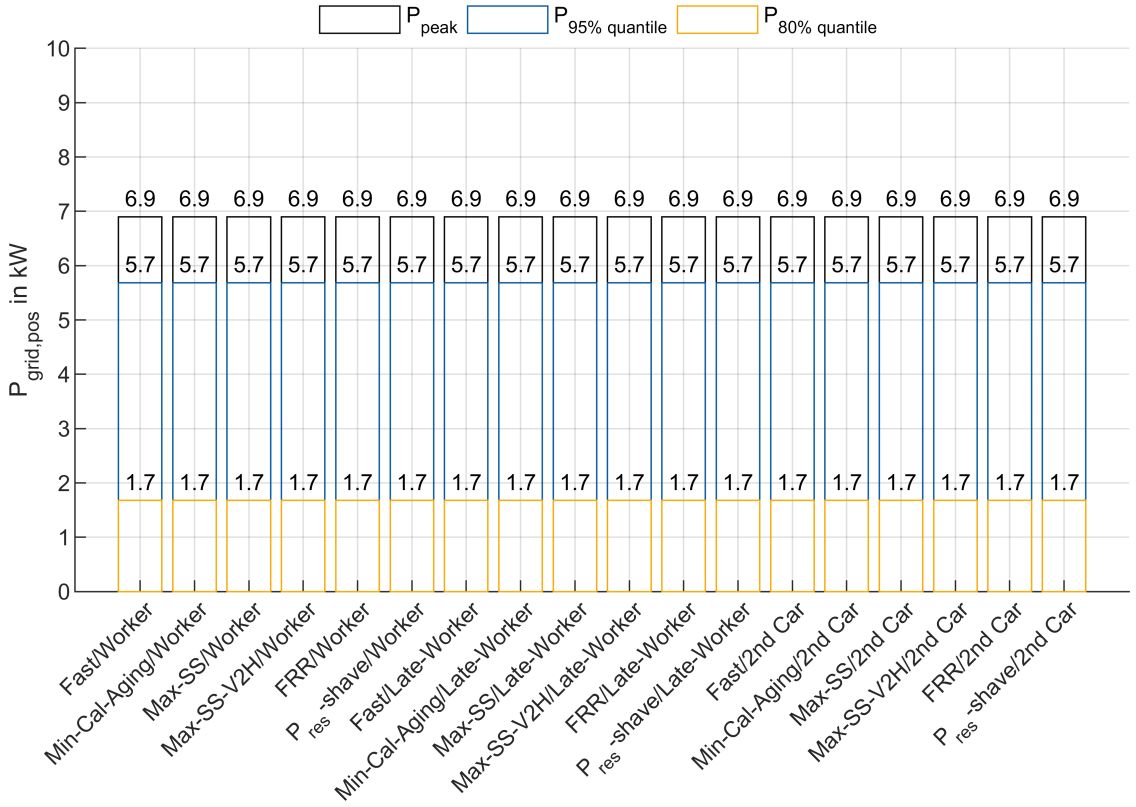

Figure A7. Positive power exchange of the household with the grid for workplace charging scenario *W* without $SoC_{V2XLimit}$.

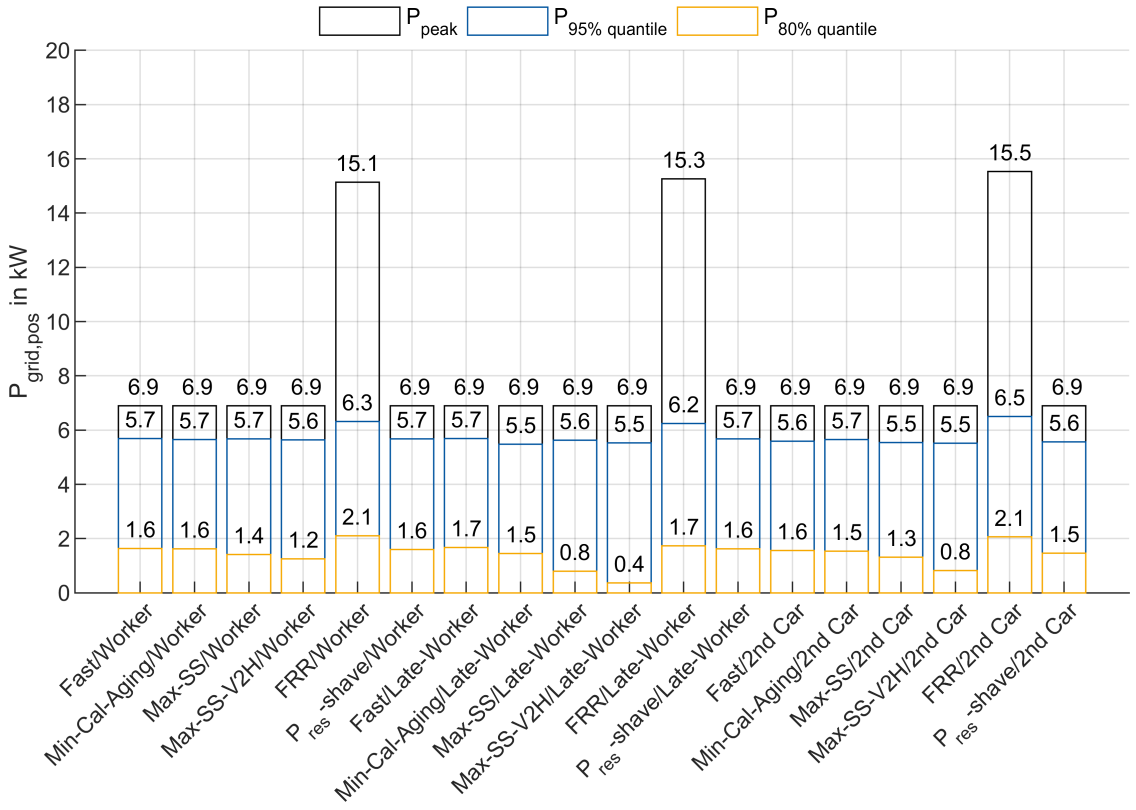

Figure A8. Positive power exchange of the household with the grid for home and workplace charging scenario *H* + *W* without $SoC_{V2XLimit}$.

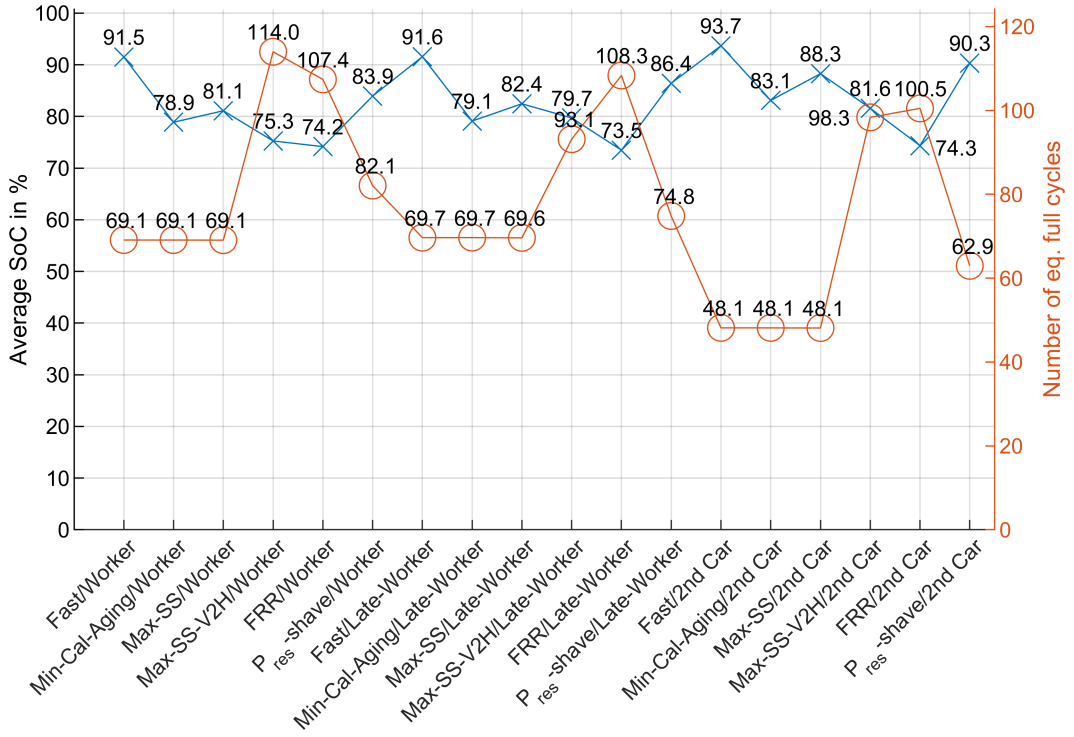

Figure A9. Average SoC and number of eq. full cycles for scenario home charging *H* and without $SoC_{V2XLimit}$

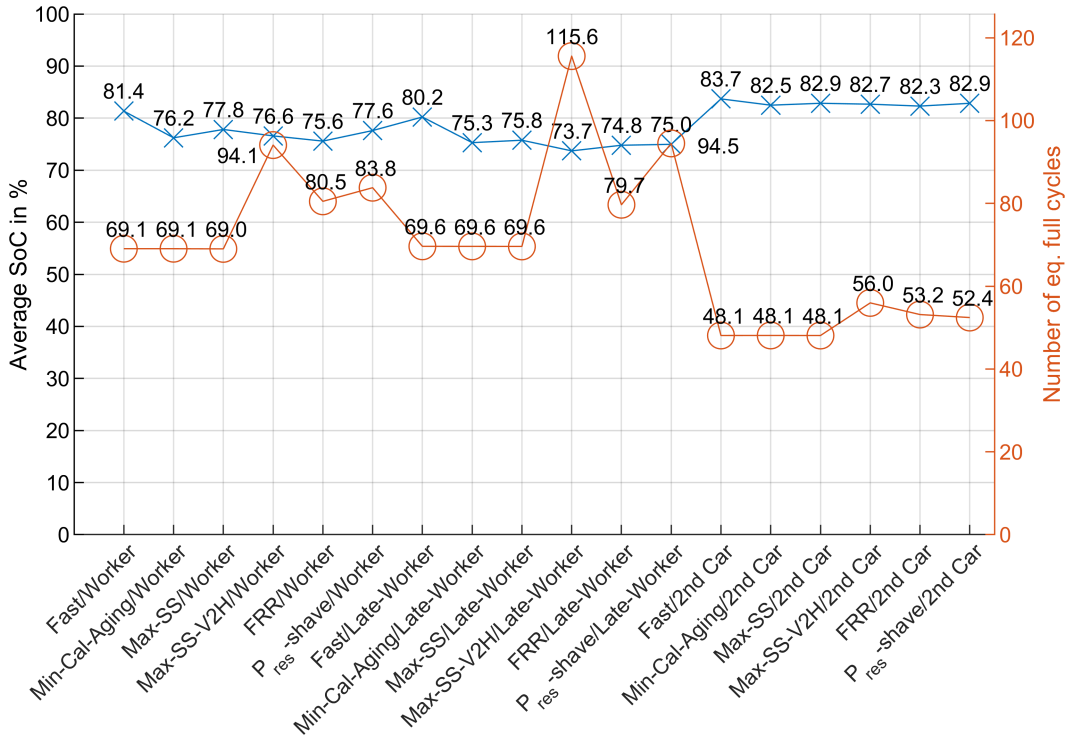

Figure A10. Average SoC and number of eq. full cycles for scenario workplace charging *W* and without $SoC_{V2XLimit}$.

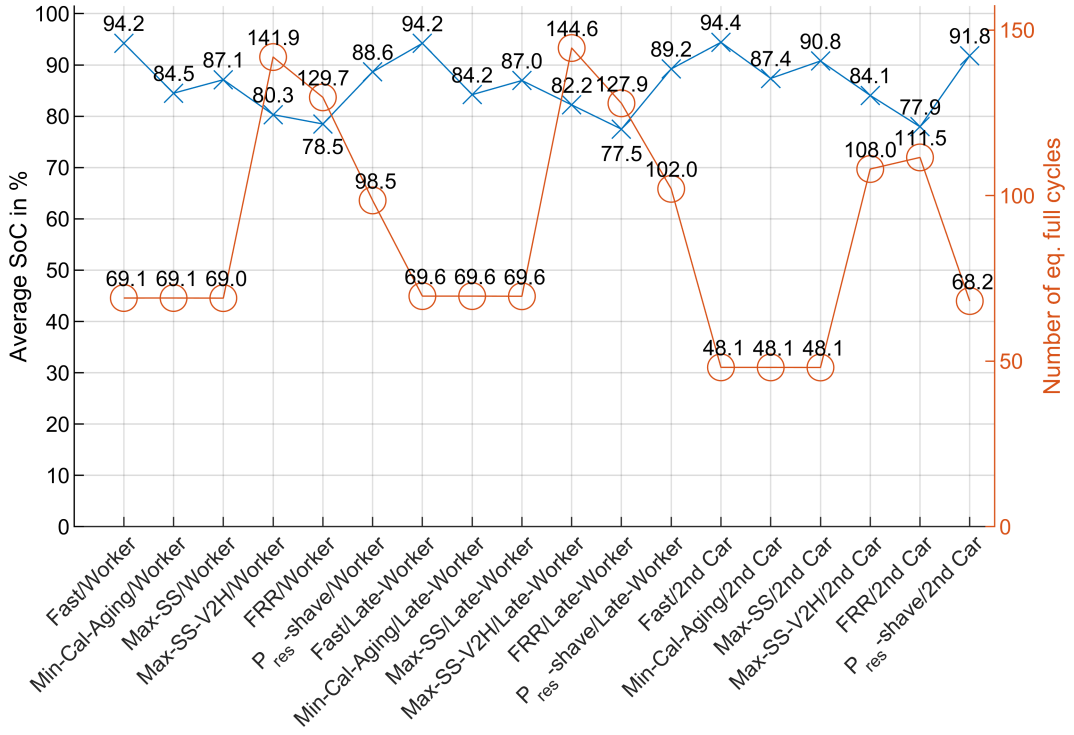

Figure A11. Average SoC and number of eq. full cycles for scenario home and workplace charging $H + W$ and no $SoC_{V2XLimit}$.

References

1. Paris Agreement. *United Nations Treaty Collection*; United Nations: New York, NY, USA, 2016 .
2. Fraunhofer ISE Energy Chart. 2020. Available online: www.energy-charts.de (accessed on 14 April 2020).
3. Dr. Harry Wirth | Fraunhofer ISE. Aktuelle Fakten zur Photovoltaik in Deutschland. 2020. Available online: www.ise.fraunhofer.de/content/dam/ise/de/documents/publications/studies/aktuelle-fakten-zur-photovoltaik-in-deutschland.pdf (accessed on 14 April 2020).
4. Merkblatt Erneuerbare Energien- KfW-Programm Erneuerbare Energien "Speicher". 25 May 2018. Available online: www.kfw.de/Download-Center/F%C3%B6rderprogramme-(Inlandsf%C3%B6rderung)/PDF-Dokumente/6000002700_M_275_Speicher.pdf (accessed on 20April 2020).
5. Angenendt, G.; Zurmühlen, S.; Axelsen, H.; Sauer, D.U. Comparison of different operation strategies for PV battery home storage systems including forecast-based operation strategies. *Appl. Energy* **2018**, *229*, 884–899. [CrossRef]
6. Schram, W.L.; Lampropoulos, I.; van Sark, W.G. Photovoltaic systems coupled with batteries that are optimally sized for household self-consumption: Assessment of peak shaving potential. *Appl. Energy* **2018**, *223*, 69–81. [CrossRef]
7. Barzegkar-Ntovom, G.A.; Chatzigeorgiou, N.G.; Nousdilis, A.I.; Vomva, S.A.; Kryonidis, G.C.; Kontis, E.O.; Georghiou, G.E.; Christoforidis, G.C.; Papagiannis, G.K. Assessing the viability of Battery Energy Storage Systems coupled with Photovoltaics under a pure self-consumption scheme. *Renew. Energy* **2020**, *152*, 1302–1309. [CrossRef]
8. Munkhammar, J.; Grahn, P.; Widén, J. Quantifying self-consumption of on-site photovoltaic power generation in households with electric vehicle home charging. *Sol. Energy* **2013**, *97*, 208–216. [CrossRef]
9. Englberger, S.; Hesse, H.; Kucevic, D.; Jossen, A. A Techno-Economic Analysis of Vehicle-to-Building: Battery Degradation and Efficiency Analysis in the Context of Coordinated Electric Vehicle Charging. *Energies* **2019**, *12*, 955. [CrossRef]
10. Chakravorty, D.; Chaudhuri, B.; Hui, S.Y.R. Rapid Frequency Response From Smart Loads in Great Britain Power System. *IEEE Trans. Smart Grid* **2017**, *8*, 2160–2169. [CrossRef]

11. Litjens, G.; Worrell, E.; van Sark, W. Economic benefits of combining self-consumption enhancement with frequency restoration reserves provision by photovoltaic-battery systems. *Appl. Energy* **2018**, *223*, 172–187. [CrossRef]
12. Münderlein, J.; Steinhoff, M.; Zurmühlen, S.; Sauer, D.U. Analysis and evaluation of operations strategies based on a large scale 5 MW and 5 MWh battery storage system. *J. Energy Storage* **2019**, *24*, 100778. [CrossRef]
13. Statkraft Direktvermarkung MRL Wind Power. 2020. Available online: www.statkraftdirektvermarktung.de/pioniergeist/minutenreserveleistung-wind (accessed on 14 April 2020).
14. Next Kraftwerke VPP. Available online: www.next-kraftwerke.com/vpp/virtual-power-plant (accessed on 14 April 2020).
15. Tennet. *End Report FCR Pilot—FCR Delivery with Aggregated Assets*; TenneT TSO B.V.: Arnhem, The Netherlands, 2018.
16. Bach Andersen, P.; Hashemi Toghroljerdi, S.; Meier Sørensen, T.; Christensen, B.; Christian Morell Lodberg Høj, J.; Zecchino, A. *The Parker Project*; Technical University of Denmark, Lyngby, Denmark, 2019.
17. Olk, C.; Sauer, D.U.; Merten, M. Bidding strategy for a battery storage in the German secondary balancing power market. *J. Energy Storage* **2019**, *21*, 787–800. [CrossRef]
18. Angenendt, G.; Merten, M.; Zurmühlen, S.; Sauer, D.U. Evaluation of the effects of frequency restoration reserves market participation with photovoltaic battery energy storage systems and power-to-heat coupling. *Appl. Energy* **2020**, *260*, 114186. [CrossRef]
19. Jargstorf, J.; Wickert, M. Offer of secondary reserve with a pool of electric vehicles on the German market. *Energy Policy* **2013**, *62*, 185–195. [CrossRef]
20. 50Hertz Transmission GmbH , Amprion GmbH, TenneT TSO GmbH, TransnetBW GmbH. regelleistung.net. Available online: www.regelleistung.net/ext/tender/remark/news/433 (accessed on 8 April 2020).
21. KU Leuven Energy Institute. *Electricity_Market_Factsheet*; KU Leuven: Leuven, Belgium, 2015 . Available online: https://set.kuleuven.be/ei/factsheets (accessed on 20 April 2020).
22. EPEX Group. Available online: www.epexspot.com/en/tradingproducts-intraday-trading (accessed on 8 April 2020).
23. ENTSO-E. *Supporting Paper for the Load-Frequency Control and Reserves Network Code*; ENTSO-E: Brussels, Belgium, 28 June 2013.
24. European Comission. *COMMISSION REGULATION (EU) 2017/1485—Of 2 August 2017—Establishing a Guideline on Electricity Transmission System Operation*; European Comission, Brussels, Belgium, 2017
25. 50Hertz Transmission GmbH, Amprion GmbH, TenneT TSO GmbH, TransnetBW GmbH. regelleistung.net. Available online: www.regelleistung.net/ext/static/prl (accessed on 8 April 2020).
26. Merten, M.; Olk, C.; Schoeneberger, I.; Sauer, D.U. Bidding strategy for battery storage systems in the secondary control reserve market. *Appl. Energy* **2020**, *268*, 114951. [CrossRef]
27. Merten, M.; Rücker, F.; Schoeneberger, I.; Sauer, D.U. Automatic Frequency Restoration Reserve Market Prediction: Methodology and Comparison of Various Approaches. *Appl. Energy* **2020**, *268*, 114978. [CrossRef]
28. Magnor, D.; Gerschler, J.B.; Ecker, M.; Merk, P.; Sauer, D.U. Concept of a Battery Aging Model for Lithium-Ion Batteries Considering the Lifetime Dependency on the Operation Strategy. In Proceedings of the 24th European Photovoltaic Solar Energy Conference, Hamburg, Germany, 21–25 September 2009; pp. 3128–3134.
29. Magnor, D. *Globale Optimierung netzgekoppelter PV-Batteriesysteme unter besonderer Berücksichtigung der Batteriealterung*; RWTH Aachen: Aachen, Germany, 2017.
30. Figgener, J.; Haberschusz, D.; Kairies, K.P.; Wessels, O.; Tepe, B.; Sauer, D.-U. *Wissenschaftliches Mess- und Evaluierungsprogramm Solarstromspeicher 2.0 [Scientific Measuring and Evaluation Program for Photovoltaic Battery Systems]: Jahresbericht 2018*; ISEA Institute for Power Electronics and Electrical Drives, RWTH Aachen: Aachen, Germany, 2018.
31. European Comission. Teil III: Anleitung für die Ausführung von Normungsaufträgen. In *Leitfaden zur europäischen Normung als Unterstützung für legislative und politische Maßnahmen der Union*; European Comission: Brussels, Belgium , 2015.
32. Sauer, D.-U. Untersuchungen zum Einsatz und Entwicklung von Simulationsmodellen für die Auslegung von Photovoltaik-Systemen. Diploma Thesis, TH Darmstadt, Darmstadt, Germany, 1994.
33. Behrens, K. Horizon at station Lindenberg. 2007. Available online: https://doi.org/10.1594/PANGAEA.669521 (accessed on 20 April 2020).

34. Bost, M.; Hirschl, B.; Aretz, A. *Effekte von Eigenverbrauch und Netzparität bei der Photovoltaik—Langfassung*; Institut für ökologische Wirtschaftsforschung (IÖW) GmbH, gemeinnützig: Berlin, Germany, 2011.
35. Daimler AG. Available online: https://media.daimler.com/marsMediaSite/ko/en/9920260 (accessed on 20 April 2020).
36. infas Institut für angewandte Sozialwissenschaft GmbH. *Mobilität in Deutschland 2017—Ergebnisbericht*; BMVI: Berlin, Germany, 2017
37. Schmalstieg, J.; Käbitz, S.; Ecker, M.; Sauer, D.U. A holistic aging model for Li(NiMnCo)O2 based 18650 lithium-ion batteries. *J. Power Sources* **2014**, *257*, 325–334. [CrossRef]
38. Kost, C.; Schlegl, T.; Jülch, V.; Nguyen, H.T.; Schlegl, T. *Stromgestehungskosten erneuerbare Energien*; Fraunhofer ISE: Freiburg, Germany, March 2018.
39. Bundesnetzagentur; Bundeskartellamt. *Monitoringbericht 2019*; Bundesnetzagentur: Bonn, Germany, 2019.
40. gridX GmbH. Available online: www.gridx.de/produkt/gridbox (accessed on 13 April 2019).
41. Photovoltaikforum.com. Regelleistungsmodell von Caterva: "Für jedes Kilowatt Regelleistung 150 bis 160 Euro im Jahr". Available online: www.photovoltaikforum.com/magazin/praxis/regelleistungsmodell-von-caterva-fuer-jedes-kilowatt-regelleistung-150-bis-160-euro-im-jahr-4765/ (accessed on 13 April 2019).